ISSN 0030-6096

OSAKA CITY MEDICAL JOURNAL

Vol. 70
No. 1

2024

PUBLISHED BY
OSAKA CITY MEDICAL ASSOCIATION
OSAKA JAPAN

Osaka City Medical Journal
Vol. 70, No. 1, June 2024

CONTENTS

page

Association between Transpyloric Feeding and Chronic Lung Disease in Extremely Low Birth Weight Infants
SATOSHI OHNISHI, ERI MATSUTANI, MIHO NONOMURA, KATSUTOSHI MATSUI, MAKIKO FUYUKI, EMI TANAKA, and TAKASHI HAMAZAKI 1

Effect of Intraoperative Amino Acid Infusion on Postoperative Acute Kidney Injury after Open Abdominal Aortic Aneurysm Repair : A Retrospective Cohort Study
MASAHIRO KAZAWA, DAIJIRO KABATA, and AYUMI SHINTANI 9

—Case Report—

Multiple Cerebral Infarctions due to a Calcified Amorphous Tumor that was Surgically Resected Successfully: A Case Report
KOSUKE OKAMOTO, MAYU SHIOMI, KEISUKE TOGAWA, HIROKA SAKAGUCHI, AKITOSHI TAKEDA, TAKENOBU SHIMADA, AKIMASA MORISAKI, YUKO KUWAE, MASAHIKO OHSAWA, and YOSHIAKI ITOH 19

Jejunal Herniation into the Lesser Sac through a Defect in the Gastrocolic Ligament Diagnosed with Multidetector Computed Tomography: A Case Report
NORIKO TAKESHITA, KIYOTAKA YUKIMOTO, MASAHIRO TOKUNAGA, TOMOHIRO OHIRA, HIROYUKI MAEDA, and TOHRU TAKESHITA 27

Commando Operation with Aortic Root Replacement for a Patient with Extensive Infective Endocarditis Surrounding the Aortomitral Fibrous Continuity: Report of a Case
YASUYUKI BITO, MASANORI SAKAGUCHI, NORIAKI KISHIMOTO, AKIHIRO SUMIYA, TAKUYA MIURA, and TAKANOBU AOYAMA 35

Osaka City Med. J. Vol. 70, 1-8, 2024

Association between Transpyloric Feeding and Chronic Lung Disease in Extremely Low Birth Weight Infants

Satoshi Ohnishi[1)], Eri Matsutani[1)], Miho Nonomura[1)], Katsutoshi Matsui[1,2)], Makiko Fuyuki[1)], Emi Tanaka[1)], and Takashi Hamazaki[1)]

Department of Pediatrics[1)], Graduate School of Medicine, Osaka Metropolitan University; and Department of Neonatology[2)], Osaka City General Hospital

Abstract

Background

The management of transpyloric feeding (TPF) in preterm infants has not been thoroughly studied since the 1980s. The objective of this study was to compare the risk of chronic lung disease (CLD) or death between TPF and gastric feeding (GF) in extremely low birth weight (ELBW) infants.

Methods

This retrospective cohort study included all ELBW infants born at a single-center tertiary neonatal intensive care unit between 2017 and 2021. The primary outcome was death or CLD, and the study examined association between both nutrition methods and the prognosis of ELBW.

Results

During the study period, 60 ELBW infants were included. Baseline characteristics were similar between the two groups. Twenty-four infants received TPF. Univariate regression analysis revealed that death or CLD occurred in 41.6% and 61.1% of infants who received TPF and GF, respectively (p =0.045). Multivariate logistic regression analysis indicated that TPF (odds ratio, 0.82; 95% confidence interval, 0.8-0.9) was a significant factor that reduced the incidence of death or CLD. Growth and adverse gastrointestinal outcomes were not significantly different between the two groups.

Conclusions

TPF may decrease the risk of death or CLD in ELBW infants without significant adverse events, but larger randomized trials are needed to confirm this association.

Key Words: Chronic lung disease; Transpyloric feeding; Extremely low birth weight infants

Introduction

Chronic lung disease (CLD) is an important cause for morbidity in preterm infants, especially in

Received March 1, 2023; accepted June 13, 2023.
Correspondence to: Satoshi Ohnishi, MD, PhD.
Department of Pediatrics, Graduate School of Medicine, Osaka Metropolitan University,
1-4-3 Asahimachi, Abeno-ku, Osaka 545-8585, Japan
Tel: +81-6-6645-3816; Fax: +81-6-6636-8737
E-mail: ohnishi@omu.ac.jp

extremely low birth weight infants (ELBW). CLD is associated with serious long-term complications, including pulmonary and neurodevelopmental impairment and increased need for health and education services[1-3]. Approximately 45% of preterm infants born at <29 weeks of postmenstrual age (PMA) are diagnosed with CLD[4]. CLD is characterized by an inflammatory response causing abnormal lung development and decreased vascular and alveolar development, which requires supplemental oxygen therapy and assisted ventilation at 36 weeks of PMA[5,6]. CLD has multifactorial causes, such as chorioamnionitis (CAM), fetal growth restriction, ventilatory management, oxygen, patent ductus arteriosus (PDA), and prematurity-based malnutrition[7].

The association between gastroesophageal reflux (GER) and exacerbation of CLD in preterm infants is a controversial topic, despite reports suggesting a correlation[8-11]. It is important to note that physiological GER can develop in newborns, especially in preterm infants[12]. Additionally, mechanical ventilation during endotracheal intubation may lead to silent aspiration in preterm infants. For nutritional support, gastric feeding is generally considered less invasive and less expensive, but it carries a risk of vomiting. On the other hand, transpyloric feeding is more invasive and expensive, but it has the advantage of better nutrient absorption and a reduced risk of aspiration. Indeed, adult guidelines recommend transpyloric feeding (TPF) as an effective treatment for GER[13,14]. A meta-analysis of adults found that TPF reduces the incidence of ventilator-associated pneumonia compared to gastric feeding (GF), but no significant difference was observed in the duration of mechanical ventilation between the two groups[15]. In a small randomized controlled trial involving pediatric patients, TPF did not reduce the incidence of GER or the duration of mechanical ventilation[16]. However, a retrospective cohort study in ELBW infants found that initiating TPF within the first week of birth significantly reduced the composite outcome of death or bronchopulmonary dysplasia, which is a specific form of CLD[17]. Although there have been reports of TPF reducing short-term effects such as apnea of prematurity and bradycardia in preterm infants[18,19], there is still a lack of clinical randomized controlled trials examining the relationship between TPF and CLD in this population[20].

TPF is considered when gastric feeding is intolerable due to poor stomach emptying or severe gastroesophageal reflux. There are currently no guidelines for ELBW regarding the use of transpyloric feeding. The aim of this single-center retrospective study was to investigate whether TPF could reduce the incidence and exacerbation of CLD in ELBW infants, while also examining any potential adverse effects.

Methods

Data collection

A retrospective cohort study that included all ELBW infants admitted to the neonatal intensive care unit (NICU) at Osaka Metropolitan University Hospital (former Osaka City University Hospital), a single tertiary center in Japan, was conducted between January 2017 and December 2021. Informed consent was obtained from all parents at birth, and the study was approved by the Institutional Medical Ethics Committee (No: 2022-015; Jun 2nd, 2022). Data were collected from the medical records. The initial enrollment criterion was birth weight <1000g. Infants were excluded if they did not receive enteral feeding within the first week after birth, died prior to initiation of enteral feeding, or had a chromosomal disorder.

The following demographic and perinatal data were obtained: gestational age, birth weight, body

length, head circumference at birth, sex, mode of delivery, singleton or multiple pregnancy, 1- and 5-minute Apgar scores, antenatal steroid use, and presence of premature rupture of membrane, small for gestational age infant, histological CAM, and hypertensive disorders of pregnancy. Primary composite outcome of death or CLD. CLD was defined as providing supplemental oxygen or positive pressure and use of a high-flow nasal cannula at 36 weeks of PMA. Secondary outcomes included days requiring mechanical ventilation, enteral feeding establishment period of >100 mL/kg/day, duration of hospitalization, weight, body length, and head circumference at discharge, intraventricular hemorrhage, cystic periventricular leukomalacia, necrotizing enterocolitis (NEC), focal intestinal perforation (FIP), sepsis, need for indomethacin for symptomatic PDA, surgical PDA, and retinopathy of prematurity requiring photocoagulation. Severe CLD was defined as the requirement of 30% or more supplemental oxygen or the need for high-frequency ventilation or positive pressure at 36 weeks of PMA.

GF and TPF insertion

The attending neonatologist made individual assessments to determine the timing and duration of GF or TPF, which was initiated at their discretion during the study period. Common indications for initiating TPF included gastroesophageal reflux (GER), aspiration, and feeding intolerance.

In this study, a 3 Fr, enteral feeding tube (JMS Co., Ltd., Tokyo, Japan) was used for GF. Prior insertion positioning the patient in a semi-upright position, measuring the tube length from the nostril to the earlobe, lubricating the tube, inserting it through the nostril and directing it towards the back of the throat, verifying placement by aspirating gastric contents. For TPF, a 5 Fr, 120 cm long, weighted polyvinyl chloride, enteral feeding tube (Kangaroo; Covidien Japan, Tokyo, Japan) was used. A neonatologist inserted the transpyloric tube at the bedside using a stylet and a fluoroscope. The tube was gently guided into the duodenum and its position was confirmed by radiography before enteral feeding was replaced with a sustained infusion.

Nutritional protocols

All infants admitted to the NICU received parenteral and enteral nutrition. Amino acid solution was started at 1.5-2 g/kg/day parenterally within 24 h after birth and increased by 1 g/kg every 24 h to a maximum of 3.5 g/kg/day. The parenteral amino acid solution was gradually decreased with increasing enteral nutrition and discontinued when full enteral feeding of approximately 150 mL/kg/day was achieved. Lipid supplementation was initiated at 0.5 g/kg/day on day 3 or 4 after birth and increased by 0.5 g/kg/day to a maximum of 2 g/kg/day. Breast milk or formula feed was initiated at 5-10 mL/kg/day on day 1 after birth. When full enteral feeding was achieved, it was replaced with fortified breast milk or preterm formula.

Anthropometric measurements

Trained nurses measured the infant's length, weight, and head circumference at birth and discharge. Body weight was measured to the nearest gram using a digital electronic scale. Recumbent body length was measured using a board. While one examiner held the infant's head in a vertical position, with the top of the head touching the fixed headboard, the second examiner extended the legs and firmly placed the movable footboard against the heels. The occipitofrontal head circumference was measured by placing a tape measure firmly around the head at the most prominent part of the frontal bulge and the occiput.

Statistical analyses

Data is expressed as mean (standard deviation) or numbers (%). Continuous variables were

analyzed using unpaired Student's t-test or Mann-Whitney U test, while categorical variables were analyzed using χ^2 test or Fisher's exact test. Multivariable logistic regression was used to evaluate the odds ratios (ORs) and 95% confidence intervals (CI). All statistical analyses were performed using R (version 3.6.2; R Foundation for Statistical Computing, Vienna, Austria). Statistical significance was set at $p < 0.05$.

Results

During the study period, 60 inborn ELBW infants were admitted to the NICU of Osaka Metropolitan University Hospital. Of the 60 infants, 24 were treated with TPF and 36 were GF. No infants died prior to the initiation of enteral feeding; two infants on GF died in the hospital. The baseline characteristics are shown in Table 1. Gestational age (26.3±1.4 weeks vs 26.6±1.3 weeks) and birth weight (695.4±159.5g vs 698.2±187.1g) were similar between the two groups. There were more infants with GF who had a histological CAM than there were with TPF (p=0.04). No other significant differences were noted in baseline characteristics between the two groups.

The clinical outcomes of the study population are summarized in Table 2. Primary composite outcome of death or CLD at 36 weeks of PMA (CLD36) occurred in 41.6% and 61.1% of infants who received TPF and GF (p=0.045), respectively. Univariate regression analysis revealed that the secondary outcomes, the incidence of CLD36 and the incidence of severe CLD36, did not demonstrate a significant difference between the two groups. Other morbidities, such as NEC, FIP, sepsis, and days to enteral nutrition >100 mL/kg/day were not significantly different between the two groups. Furthermore, the duration of hospitalization and growth at discharge, including length, weight, and head circumference measurements, were not significantly different between the two groups. The time of TPF initiation was approximately 20.3±13.2 days after birth, and the TPF duration was 33.1±29.7 days.

Table 1. Characteristics of the study population

	TPF (n=24)	GF (n=36)	p value
Gestational age (weeks)	26.3 (1.4)	26.6 (1.3)	0.24
Birth weight (g)	695.4 (159.5)	698.2 (187.1)	0.96
SGA	12 (50.0%)	20 (55.6%)	0.62
1-min Apgar score	3.8 (2.2)	3.9 (2.2)	0.87
5-min Apgar score	6.6 (1.8)	6.7 (2.0)	0.84
Male	10 (41.6%)	20 (55.6%)	0.35
Antenatal steroid	21 (87.5%)	27 (75.0%)	0.43
PROM	3 (12.5 %)	2 (5.6%)	0.24
Histological CAM	9 (37.5%)	17 (47.2%)	0.04*
HDP	7 (29.1%)	8 (22.2%)	0.73
Multiple pregnancy	4 (16.7%)	9 (25.0%)	0.73
Caesarian delivery	18 (75.0%)	32 (88.9%)	0.54
Body length at birth (cm)	30.8 (2.4)	30.2 (3.4)	0.5
Head circumference at birth (cm)	23.0 (1.7)	23.2 (1.3)	0.72

Variables are mean (standard deviation) or number (%). *Statistically significant. Abbreviations: TPF, transpyloric feeding; GF, gastric feeding; SGA, small for gestational age; PROM, premature rupture of the membranes; CAM, chorioaminionitis; and HDP, hypertensive disorders of pregnancy.

Since the univariate analysis revealed that TPN reduced death or incidence of CLD36, we attempted a multiple regression analysis with TPN and other factors that could influence the composite outcome of death or CLD36. The factors used in the multiple regression analysis were TPF, histological CAM, gestational age, sex, symptomatic PDA, and PDA operation. As the results, TPF (OR, 0.82; 95% CI, 0.8-0.9; p=0.048) was a significant factor in reducing death or CLD36 (Table 3).

Table 2. Clinical outcomes of the study population

	TPF (n=24)	GF (n=36)	p value
Death	0	2 (5.6%)	0.45
Death or CLD36	10 (41.6%)	22 (61.1%)	0.045*
CLD28	23 (95.8%)	29 (80.5%)	0.16
CLD36	10 (41.6%)	20 (56%)	0.09
severe CLD36	3 (12.5%)	6 (16.7%)	0.21
Symptomatic PDA	18 (75.0%)	32 (88.9%)	0.43
IVH	2 (8.3%)	0	0.43
Cystic PVL	0	2 (5.6%)	0.45
NEC	1 (4.2%)	2 (5.6%)	1
FIP	0	4 (11.1%)	0.19
Sepsis	3 (12.5%)	2 (5.6%)	0.61
ROP	7 (29.2%)	10 (27.8%)	0.54
Mechanical ventilation (days)	25.8 (14.3)	21.2 (18.7)	0.38
TPF initiation (days)	20.3 (13.2)	NA	
TPF duration (days)	33.1 (29.7)	NA	
Days to enteral nutrition establishment >100 mL/kg/d (days)	12.2 (3.0)	13.4 (3.7)	0.31
Period of hospitalization (days)	102.1 (23.8)	103.2 (35.8)	0.91
Weight at discharge (g)	2837.4 (570.4)	2711.1 (781.5)	0.59
Body length at discharge (cm)	45.6 (3.7)	46.0 (5.5)	0.77
Head circumference at discharge (cm)	34.0 (2.2)	34.3 (2.5)	0.68

Variables are mean (standard deviation) or number (%). *Statistically significant. Abbreviations: TPF, transpyloric feeding; GF, gastric feeding; CLD36, chronic lung disease at 36 weeks of postmenstrual age; CLD28, chronic lung disease at 28 weeks of postmenstrual age; PDA, patent ductus arteriosus; IVH, intraventricular hemorrhage; PVL, periventricular leukomalacia; NEC, necrotizing enterocolitis; FIP, focal intestinal perforation; and ROP, retinopathy of prematurity.

Table 3. Multivariate logistic regression analysis for factors affecting death or CLD36

	Odds ratio	95% CI	p value
TPF	0.82	0.8-0.9	0.048*
Histological CAM	1.1	0.9-12.5	0.06
Gestational age (weeks)	0.6	0.4-0.9	0.035*
Male	4.4	1.1-13.6	0.043*
Symptomatic PDA	0.4	0.06-2.4	0.31
PDA operation	3.7	1.3-8.3	0.045*

*Statistically significant. Abbreviations; CLD36, chronic lung disease severity classification at 36 weeks-postmenstrual age; CI, confidence intervals; TPF, transpyloric feeding; CAM, chorioamnionitis; and PDA, patent ductus arteriosus.

Discussion

In the present study, multivariate regression analyses revealed that ELBW infants treated with TPF were associated with a reduced risk of composite outcomes of death or CLD than infants treated with GF. Furthermore, growth and adverse gastrointestinal outcomes were not significantly different between the two groups. Our results highlight the need to reassess the usefulness of TPN for ELBW infants. The reduction of CLD not only improves long-term respiratory health but also lowers the risk of neurological disorders, such as cerebral palsy and cognitive impairment.

Over the past several decades, various strategies have been designed to eliminate lung injury and decrease mortality in extremely premature infants worldwide. While CAM is a known risk factor for bronchopulmonary dysplasia in preterm infants[21], our results suggest that the presence of histological CAM was not associated with an increased risk of composite outcomes of death or CLD36.

Pulmonary aspiration remains an unresolved cause of lung injury in preterm infants. Farhath et al serially collected 239 tracheal aspirate samples from 45 ELBW infants on mechanical ventilation. They detected pepsin, an indicator of stomach contents, in over 92% of the samples, with higher levels in fed infants[22]. In the same research group, it was observed that the concentration of pepsin in the tracheal aspirate of preterm infants who developed bronchopulmonary dysplasia or died before 36 weeks of PMA was significantly elevated[9]. Aspiration has been specifically noted in preterm infants due to factors such as immature lower esophageal sphincter tone, delayed gastric emptying, and the use of endotracheal tubes without cuffs[26].

TPF was once a commonly performed strategy to reduce aspiration risk in NICUs. However, safety concerns led to its discontinuation in the 1980s[20,23-25], and it became a treatment of the past despite its potential benefits. While McGuire et al reported a significant increase in mortality due to TPF because of a greater incidence of gastrointestinal disturbances[27], our institution has been using TPF for a long time without experiencing any adverse events, such as gastric or intestinal perforation and NEC. We were able to place a TPF tube without gastric perforation by carefully guiding the tube tip along the gastric curvature from the abdominal wall. This technical improvement may contribute to a better outcome in the TPF group.

In a systematic review conducted by Watson et al in 2013, they concluded that the effectiveness of TPF could not be proven based on the analysis of nine clinical studies. However, they also noted that there was a lack of high-quality studies, such as randomized controlled trials, and that each of the clinical studies analyzed had methodological issues that required cautious interpretation[20]. A retrospective study by Wallenstein et al showed that in ELBW infants, the composite outcome of death or CLD was significantly reduced in ELBW infants initiated with early TPF within the first week after birth than in those with GF (58% vs 67%, OR: 0.6, 95% CI; 0.3-0.9)[17]. No significant difference was observed in CLD alone between the two groups. Findings of our study support those of Wallenstein et al, and provide additional evidence that TPF is effective in reducing the risk of death or CLD. Unlike Wallenstein et al, who initiated TPF within the first week of life, our study included ELBW infants who received late TPF to evaluate its outcomes and produced comparative results. Our study could not clarify the efficacy of TPF during the early or subacute-to-chronic period. Despite advances in neonatal care, such as the use of antenatal steroids and improved respiratory management, lung injury caused by aspiration continues to be a challenge. As Wallenstein et al have stated, it is necessary to revisit the potential benefits of TPF[28].

This study has several limitations. The small sample size reduces the credibility of the statistical

evaluation. In addition, the study was conducted at a single-center NICU with unique management practices, limiting the generalizability of the findings. Neonatologists made the choice between TPF and GF based on their clinical judgment, creating a bias due to the lack of established criteria. The timing of TPF initiation varied between the early and late TPF groups, making it unclear which, if either, group was effective. Finally, the study was retrospective in design, highlighting the need for prospective randomized trials to externally validate these findings.

In conclusion, the potential association between TPF and a decreased risk of death or CLD in ELBW infants suggests the need to reevaluate the use of TPF in this high-risk population prone to aspiration.

Acknowledgements

All authors have no COI to declare regarding the present study.

References

1. Doyle LW, Anderson PJ. Long-term outcomes of bronchopulmonary dysplasia. Semin Fetal Neonatal Med 2009; 14:391-395.
2. Schmidt B, Asztalos EV, Roberts RS, et al. Impact of bronchopulmonary dysplasia, brain injury, and severe retinopathy on the outcome of extremely low-birth-weight infants at 18 months: results from the trial of indomethacin prophylaxis in preterms. JAMA 2003;289:1124-1129.
3. Vohr BR, Wright LL, Poole WK, et al. Neurodevelopmental outcomes of extremely low birth weight infants <32 weeks' gestation between 1993 and 1998. Pediatrics 2005;116:635-643.
4. Stoll BJ, Hansen NI, Bell EF, et al. Trends in care practices, morbidity, and mortality of extremely preterm neonates, 1993-2012. JAMA 2015;314:1039-1051.
5. Hayes D Jr, Feola DJ, Murphy BS, et al. Pathogenesis of bronchopulmonary dysplasia. Respiration 2010;79:425-436.
6. Jobe AH, Bancalari E. Bronchopulmonary dysplasia. Am J Respir Crit Care Med 2001;163:1723-1729.
7. Baraldi E, Filippone M. Chronic lung disease after premature birth. N Engl J Med 2007;357:1946-1955.
8. Jolley SG, Herbst JJ, Johnson DG, et al. Esophageal pH monitoring during sleep identifies children with respiratory symptoms from gastroesophageal reflux. Gastroenterology 1981;80:1501-1506.
9. Farhath S, He Z, Nakhla T, et al. Pepsin, a marker of gastric contents, is increased in tracheal aspirates from preterm infants who develop bronchopulmonary dysplasia. Pediatrics 2008;121:e253-259.
10. Akinola E, Rosenkrantz TS, Pappagallo M, et al. Gastroesophageal reflux in infants <32 weeks gestational age at birth: lack of relationship to chronic lung disease. Am J Perinatol 2004;21:57-62.
11. Nobile S, Noviello C, Cobellis G, et al. Are infants with bronchopulmonary dysplasia prone to gastroesophageal reflux? A prospective observational study with esophageal pH-impedance monitoring. J Pediatr 2015;167:279-285.
12. Eichenwald EC. Diagnosis and management of gastroesophageal reflux in preterm infants. Pediatrics 2018;142: e20181061.
13. McClave SA, Taylor BE, Martindale RG, et al. Guidelines for the provision and assessment of nutrition support therapy in the adult critically ill patient: Society of Critical Care Medicine (SCCM) and American Society for Parenteral and Enteral Nutrition (A. S. P. E. N). JPEN J Parenter Enteral Nutr 2016;40:156-211.
14. Singer P, Blaser AR, Berger MM, et al. ESPEN guideline on clinical nutrition in the intensive care unit. Clin Nutr 2019;38:48-79.
15. Li Z, Qi J, Zhao X, et al. Risk-benefit profile of gastric vs transpyloric feeding in mechanically ventilated patients: a meta-analysis. Nutr Clin Pract 2016;31:91-98.
16. Meert KL, Daphtary KM, Metheny NA. Gasrtic vs small-bowel feeding in critically ill children receiving mechanical ventilation: a randomized controlled trial. Chest 2004;126:872-878.
17. Wallenstein MB, Brooks C, Kline TA, et al. Early transpyloric vs gastric feeding in preterm infants: a retrospective cohort study. J Perinatol 2019;39:837-841.
18. Malcolm WF, Smith PB, Mears S, et al. Transpyloric tube feeding in very low birthweight infants with suspected gastroesophageal reflux: impact on apnea and bradycardia. J Perinatol 2009;29:372-375.
19. Misra S, Macwan K, Albert V. Transpyloric feeding in gastroesophageal-reflux-associated apnea in premature

infants. Acta Paediatr 2007;96:1426-1429.
20. Watson J, McGuire W. Transpyloric versus gastric tube feeding for preterm infants. Cochrane Database Syst Rev 2013;2013:CD003487.
21. Villamor-Martinez E, Álvarez-Fuente M, Ghazi AMT, et al. Association of chorioamnionitis with bronchopulmonary dysplasia among preterm infants: a systematic review, meta-analysis, and metaregression. JAMA Netw Open 2019;2:e1914611.
22. Farhath S, Aghai ZH, Nakhla T, et al. Pepsin, a reliable marker of gastric aspiration, is frequently detected in tracheal aspirates from premature ventilated neonates: relationship with feeding and methylxanthine therapy. J Pediatr Gastroenteral Nutr 2006;43:336-341.
23. Laing IA, Lang MA, Callaghan O, et al. Nasogastric compared with nasoduodenal feeding in low birthweight infants. Arch Dis Child 1986;61:138-141.
24. Macdonald PD, Skeoch CH, Carse H, et al. Randomized trial of continuous nasogastric, bolus nasogastric, and transpyloric feeding in infants of birth weight under 1400 g. Arch Dis Child 1992;67:429-431.
25. Pereira GR, Lemons JA. Controlled study of transpyloric and intermittent gavage feeding in the small preterm infant. Pediatrics 1981;67:68-72.
26. Omari TI, Barnett CP, Benninga MA, et al. Mechanisms of gastro-esophageal reflux in preterm and term infants with reflux disease. Gut 2002;51:475-479.
27. McGuire W, McEwan P. Systematic review of transpyloric versus gastric tube feeding for preterm infants. Arch Dis Child Fetal Neonatal Ed 2004;89:F245-248.
28. Wallenstein MB, Stevenson DK. Need for reassessment of early transpyloric feeding in preterm infants. JAMA Pediatr 2018;172:1004-1005.

Osaka City Med. J. Vol. 70, 9-17, 2024

Effect of Intraoperative Amino Acid Infusion on Postoperative Acute Kidney Injury after Open Abdominal Aortic Aneurysm Repair: A Retrospective Cohort Study

Masahiro Kazawa[1,2], Daijiro Kabata[2], and Ayumi Shintani[2]

Department of Critical Care Medicine[1], National Cerebral and Cardiovascular Center ; and Department of Medical Statistics[2], Graduate School of Medicine, Osaka Metropolitan University

Abstract

Background

Acute kidney injury (AKI) is one of the serious complications after open abdominal aortic aneurysm (AAA) repair. It has been suggested that amino acid infusion may inhibit AKI. Therefore, we hypothesized that intraoperative amino acid infusion, which was used to maintain body temperature, is associated with a lower incidence of AKI.

Methods

In this retrospective, observational, single-center cohort study, we included patients who underwent AAA repair between January 2007 and April 2019. Perioperative data were extracted from medical records. The primary outcome was AKI diagnosed according to Kidney Disease: Improving Global Outcomes criteria. We estimated the effect of amino acid infusion on AKI using a multivariable Cox proportional-hazard regression analysis. As a sensitivity analysis, we estimated the effect among the matched cohort based on the propensity score.

Results

A total of 697 patients were included in the analysis, of whom 310 received amino acids infusion of around 20g. The incidence of AKI was 23.5% in the amino acid group and 19.1% in the control group. Statistical analysis did not show a significant association between amino acid administration and AKI (adjusted hazard ratios [95% confidence interval] were 0.79 [0.44-1.41] on the multivariable regression model and 0.89 [0.51-1.53] on the propensity score matching methods).

Conclusions

The effect of amino acids on AKI was not observed in our study. In our study, the dosage of amino acids administrated was significantly lower than the typical usage. Therefore, additional study is required to assess the effect of the adequate dosage of amino acids.

Key Words: Acute kidney injury; Amino acid; Open abdominal aortic aneurysm repair

Received August 14, 2023; accepted November 28, 2023.

Correspondence to: Ayumi Shintani, MPH, PhD.
Department of Medical Statistics, Graduate School of Medicine, Osaka Metropolitan University,
1-4-3 Asahimachi, Abeno-ku, Osaka 545-8585, Japan
Tel: +81-6-6645-3894; Fax: +81-6-6646-6479
E-mail: ayumi.shintani@gmail.com

Introduction

Acute kidney injury (AKI) is one of the most common complications after open repair of abdominal aortic aneurysms (AAAs). The incidence of AKI was 20%-37.3%[1-6], which is higher than the incidence of AKI after general surgery (1.0%)[7]. There are not enough reliable methods to prevent postoperative AKI, even though it is associated with an increase in long-term mortality rates with 5-year cohort survival rate of 54% respectively[8].

The effect of amino acid infusion on renal function has been previously reported; amino acid intake decreases renal vascular resistance and increases renal blood flow[9-12]. These effects have been attributed to the role of endothelium-derived nitric oxide promoted by amino acids[13]. It is known that aortic declamping in open AAA repair causes renal ischemia-reperfusion injury, resulting in reduced renal blood flow due to impaired nitric oxide synthesis and triggering AKI[14]. Therefore, it was suggested that amino acid infusion may suppress AKI after open AAA repair.

Amino acids are often administered during general anesthesia to prevent hypothermia. Since that amino acid infusion is not intended to prevent AKI, the association between amino acid infusion and AKI can be investigated retrospectively. To examine this hypothesis, we conducted a retrospective observational cohort study.

Methods

Ethical considerations

This study was approved by the ethics committee in National Cerebral and Cardiovascular Center (registration number: R19068). The ethics committee granted a waiver of signed consent because of the retrospective nature of the study.

Study design

This retrospective, observational, single-center cohort study enrolled consecutive patients who underwent open AAA repair from January 2007 to April 2019 at National Cerebral and Cardiovascular Center. Only first-time and planned operations were included. The exclusion criteria were preoperative estimated glomerular filtration rate (eGFR) $<$15 mL/min/1.73 m^2.

Surgical indications and procedure

Surgical indications were based on the 2011 Japanese Circulation Society Guidelines for Diagnosis and Treatment of Aortic Aneurysm and Aortic Dissection[15], as follows: a maximal transverse diameter $\geqq$55 mm in males and $\geqq$50 mm in females, an increase in the transverse diameter $\geqq$5 mm/6 months, or an infected aneurysm.

For AAA, open repair was generally performed at our institution; however, the vascular team considered endovascular aneurysm repair (EVAR) if the AAA satisfied any of the following conditions: anatomical characteristics that made EVAR favorable[15], age $>$75 years, history of open abdominal surgery, and history of smoking.

The surgical procedure was conducted in the following manner: Following a median abdominal incision, the surgical field was exposed. Heparin was administered at a dosage of 100 U/kg, and once it was confirmed that the activated clotting time exceeded 250 seconds, clamping was applied to both the distal and proximal segments of the aneurysm, leading to the excision of the aneurysm. Subsequently, anastomosis was performed between the artificial vessel and both the proximal and distal segments of the artery. After neutralizing the effects of heparin with protamine, the surgical incision was closed. No renal protection solution was utilized during the procedure.

Anesthetic management

In all patients, general anesthesia was performed with concomitant electrocardiography, pulse oximetry, non-invasive blood pressure measurement, and capnometry. An arterial cannula was inserted in the radial artery and a central venous catheter was inserted into the jugular vein. Arterial pressure and central venous pressure were continuously monitored. Anesthesia was managed by the attending anesthesiologist. Epidural anesthesia was also performed unless patients had a low platelet count or coagulopathy, or were undergoing antiplatelet or anticoagulation therapy. Patients were transferred to the surgical intensive care unit after open AAA repair.

The attending anesthetist decided on the infusion of amino acids. The amino acid preparation consisted of a standard mixture of amino acids (AMIPAREN Injection; Otsuka Pharmaceutical).

Diagnostic criteria for AKI

The diagnostic criteria for AKI were as follows, based on Kidney Disease Improving Global Outcomes (KDIGO) criteria: an increase in serum creatinine of ≧0.3 mg/dL within 48 hours or an increase in serum creatinine to ≧1.5 times baseline within 7 days after the surgery[16]. Baseline creatinine was defined as the most recent creatinine value before surgery.

Data acquisition

We retrospectively collected the following data from medical records: age, sex, height, weight, American Society of Anesthesiologist physical status, location of cross-clamp, anesthesia methods, anesthesia time, date of surgery, intraoperative volume of amino acids administered, minimum body temperature during surgery, the most recent pre-operative serum creatinine value, and the daily serum creatinine values until day 7 after the surgery.

Statistical analysis

Continuous variables were summarized utilizing medians and interquartile ranges. Categorical and ordinal variables were presented as frequencies and corresponding percentages.

Kaplan-Meier estimates were computed to show the cumulative incidence of AKI for patients with and without amino acid infusion after the surgery. Additionally, the influence of amino acid infusion on AKI was quantified through hazard ratios using a multivariable Cox proportional hazards regression analysis. Patients were followed for 7 days for the occurrence of AKI after the surgery. Baseline covariates, age, sex, body mass index (BMI), baseline serum creatinine level, location of cross-clamp, anesthesia time, and operation year, were adjusted for in the analysis. To assess non-linear effects of continuous variables on the outcome, restricted cubic spline functions were employed. To assess whether the effect of the amino acids infusion is modified by patients' characteristics, cross-product terms involving the presence or absence of amino acids and age, BMI, and baseline serum creatinine levels were incorporated into the regression model separately along with other baseline factors. Intraoperative fluid and blood transfusion volume were considered to strongly influence AKI although these variables were omitted as covariates due to possible multicollinearity with anesthesia time. In order to further assess the robustness of the analysis, we conducted secondary analysis to the above with adding intraoperative fluid and blood transfusion volume to the set of covariates.

As part of a sensitivity analysis, a propensity score matching was used to further eliminate the effect of the set of baseline confounding factors. Propensity scores were calculated as the estimated probability of using amino acids infusion using a logistic regression model as a function of the baseline confounding factors.

In addressing missing data, the multiple imputation method was employed. The statistical

analysis was performed across five imputed datasets, with results synthesized using Rubin's rule to calculate point estimates and confidence intervals[17]. All statistical analyses were performed using two-sided tests at the 5% significance level using R software version 4.2.2 (www.r-project.org).

Results

We used a surgical database to collect data from 709 patients who underwent planned open AAA repairs. Due to their preoperative eGFR, 12 patients were excluded and 697 patients were included in the analysis (Fig. 1). Amino acids were given to 310 (44.5%) of the patients in the study. Most patients who received infused amino acids received a dose of 20g. The baseline characteristics of the study participants are listed in Table 1. Intraoperative minimum body temperatures were comparable between the two groups (control group vs amino acid group (median [interquartile range]); 35.42℃ [34.90, 35.81] vs 35.20℃ [34.75, 35.73]) (Table 2).

The incidence of AKI within 7 days after surgery was 23.5% in the amino acid group and 19.1% in the control group. Statistical analysis failed to show a significant association between amino acid administration and AKI (adjusted hazard ratio, 0.79; 95% confidence interval, 0.44-1.41; p=0.94) (Fig. 2). Furthermore, the effect modification of the presence or absence of amino acids by each covariate, age, BMI, and baseline serum creatinine levels, was not statistically significant (Fig. 3). Within various subgroups, no significant association emerged between amino acid administration and AKI (Fig. 4).

After reducing imbalances of the potential confounding factors through the propensity score matching method, a similar result was obtained (hazard ratio, 0.89; 95% confidence interval, 0.51-1.53; p=0.66); (hazard ratio, 0.84; 95% confidence interval, 0.48-1.48; p=0.55) with adding intraoperative fluid and blood transfusion volume. The utilization of propensity score matching was validated by demonstrating the alignment of background factors between the two groups (Table 1).

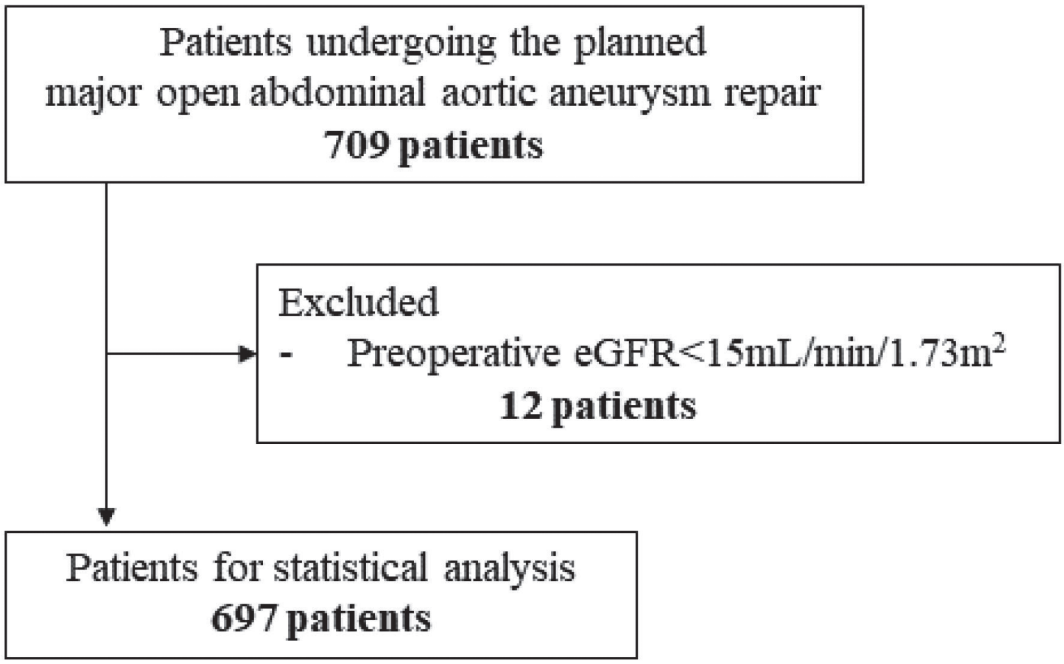

Figure 1. Recruitment flow diagram. eGFR, estimated Glomerular Filtration Rate.

Table 1. Distribution of patients' characteristics before and after propensity score matching

(a)

	Original cohort			
	Control group (N=387)	Amino acid group (N=310)	SMD	Missing (%)
Age, y	71.00 [65.00, 76.00]	71.00 [65.00, 76.00]	0.04	0
Sex, male	85.5 (331)	86.1 (267)	0.017	0
BMI, kg/m^2	23.34 [21.25, 25.40]	23.50 [21.39, 25.06]	0.028	1.6
Location of cross-clamp			0.207	1
Infrarenal	85.6 (327)	79.9 (246)		
Hemirenal	7.3 (28)	13.6 (42)		
Suprarenal	7.1 (27)	6.5 (20)		
ASA-PS			0.138	3.7
1	1.1 (4)	2.6 (8)		
2	82.5 (298)	82.9 (257)		
3	16.1 (58)	14.5 (45)		
4	0.3 (1)	0.0 (0)		
Anesthesia time, min	301.00 [260.50, 344.00]	332.50 [290.25, 390.75]	0.529	0
Preoperative creatinine, mg/dL	0.91 [0.78, 1.08]	0.97 [0.83, 1.13]	0.111	0
Operation year	2010.00 [2008.00, 2011.00]	2015.00 [2013.00, 2017.00]	1.838	0

(b)

	Matched cohort			
	Control group (N=118)	Amino acid group (N=118)	SMD	Missing (%)
Age, y	70.50 [67.00, 76.75]	71.00 [67.00, 78.00]	0.007	0
Sex, male	89.0 (105)	86.4 (102)	0.007	0
BMI, kg/m^2	23.64 [21.80, 25.56]	23.38 [21.06, 25.38]	0.078	0.4
Location of cross-clamp			0.134	1.3
Infrarenal	80.3 (94)	83.6 (97)		
Hemirenal	11.1 (13)	11.2 (13)		
Suprarenal	8.5 (10)	5.2 (6)		
ASA-PS			0.023	0
1	0.8 (1)	0.8 (1)		
2	83.1 (98)	83.9 (99)		
3	16.1 (19)	15.3 (18)		
4	0.0 (0)	0.0 (0)		
Anesthesia time, min	324.50 [292.00, 365.75]	324.00 [289.25, 380.25]	0.02	0
Preoperative creatinine, mg/dL	0.95 [0.80, 1.10]	0.96 [0.82, 1.10]	0.001	0
Operation year	2013.00 [2011.00, 2015.00]	2013.00 [2011.00, 2014.75]	<0.001	0

Propensity score matching was performed to align background factors between the two groups. Medians and interquartile ranges are presented for continuous variables, and frequency and proportions (%) of each category are presented for categorical variables. Percentages in categorical variables represent proportions of the population excluding any missing values. SMD, standardized mean difference; and ASA-PS, American Society of Anesthesiologists' physical status.

Table 2. Other characteristics not used for matching

	Control group (N=387)	Amino acid group (N=310)	P value
Operation time, min	207.00 [169.50, 247.00]	244.50 [199.50, 300.00]	<0.001
Minimum body temperature, ℃	35.42 [34.90, 35.81]	35.20 [34.75, 35.73]	0.013
Postoperative maximum creatinine, mg/dL	1.02 [0.86, 1.37]	1.15 [0.95, 1.43]	0.001
Intraoperative fluid, mL	3000.00 [2000.00, 3750.00]	4025.00 [3150.00, 5150.00]	<0.001
Intraoperative transfusion, mL	910.00 [280.00, 1560.00]	1300.00 [700.00, 2437.25]	<0.001

The values in the table represent the median and quartile range. P values were calculated by Student's T test.

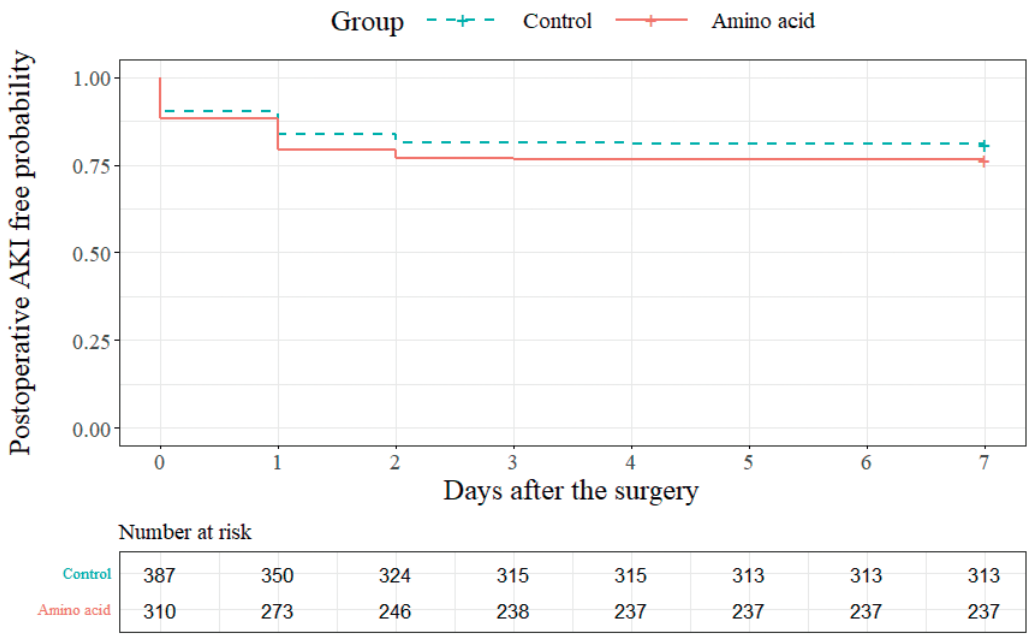

Figure 2. Kaplan-Meier curves of time to AKI. The cumulative proportion of patients with being free from the occurrence of AKI was shown using Kaplan-Meier curves comparing patients with and without the amino acid infusion. AKI, acute kidney injury.

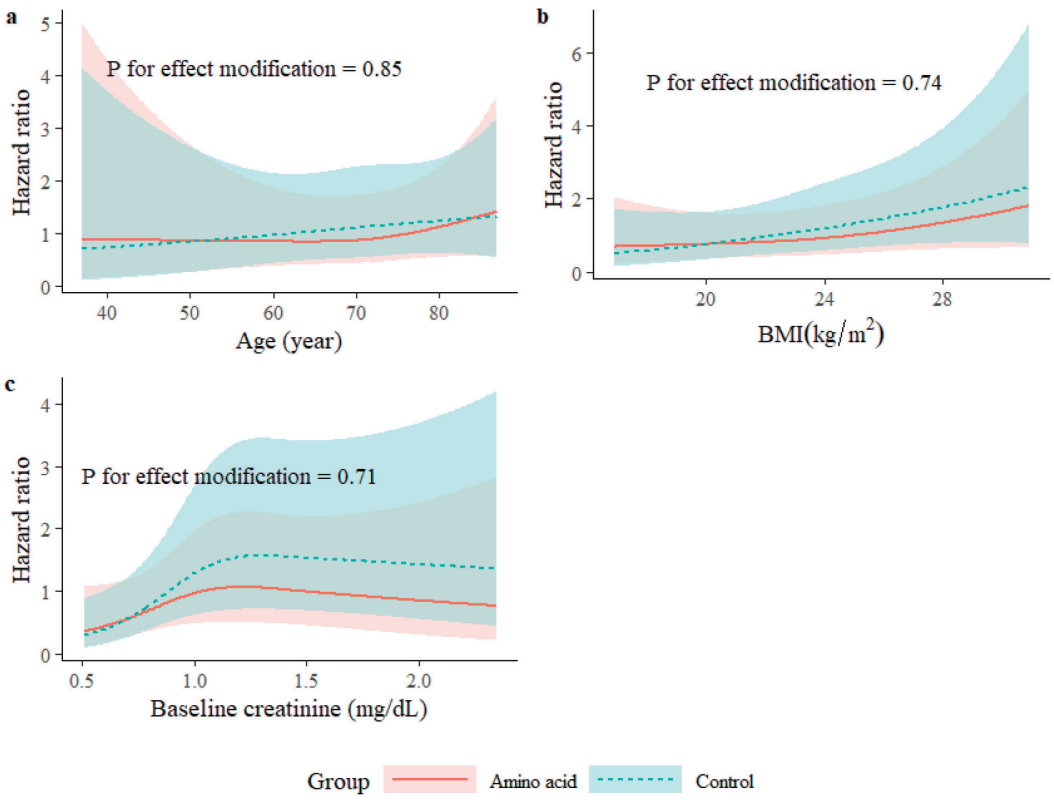

Figure 3. Assessment of effect modification of the presence or absence of amino acids by each covariate. The effect modification of the presence or absence of amino acid infusion was assessed using the multivariable Cox proportional-hazard regression model including the cross-product term between the amino acid infusion indicator and (a) age, (b) BMI, and (c) baseline serum creatinine value, separately. BMI, body mass index.

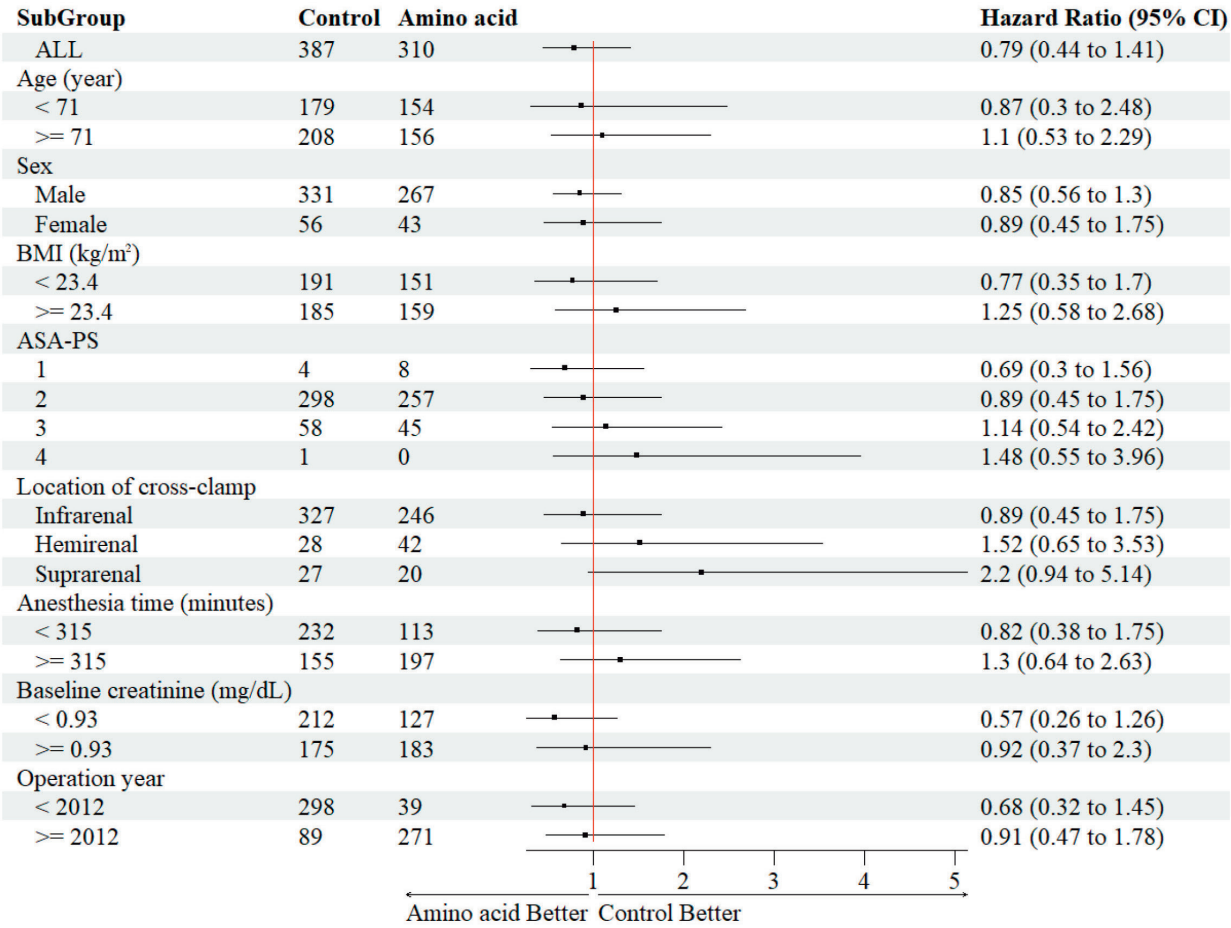

Figure 4. Forest plot of primary outcome according to subgroups. The effect of amino acids infusion was assessed in each subgroup of patients defined by baseline characteristics. For continuous baseline variables, the subgroups were classified by dividing the cohort by the median value of each variable. CI, confidence interval; BMI, body mass index; and ASA-PS, American Society of Anesthesiologists physical status.

Discussion

This study examined the effect of intraoperative amino acid infusion on the incidence of AKI. The incidence of AKI with open AAA repair was 21.1% in this study. This result was compatible with previous reports[1-6]. Our analysis did not show a statistically significant association between amino acid infusion and the incidence of AKI, and the results were similar in the sensitivity analysis using propensity scores. The baseline variables background factors employed for propensity score matching were consistent with those used in the main analysis, which involved a multivariate Cox proportional hazards analysis. Both in the multivariate Cox proportional hazards analysis and propensity score matching including intraoperative fluid and blood transfusion volume as covariates the results remained consistent with the initial findings. Irrespective of the analytical method employed, the direction of the effects remained consistent with prior studies.

One reason that amino acid infusion had a small effect on the incidence of AKI might be the low dose of amino acids administered. The median dose of amino acids in our study was 20g. This amount is much smaller than in a previous study in which 100g of amino acids were administered daily[18]. Another study showed that there was a dose-response relationship between physiological increments in plasma amino acid concentrations and the stimulation of GFR and renal blood flow[19].

A threefold increase in plasma amino acid concentrations resulted in maximum GFR and renal blood flow increases of 22% and 27%, respectively. Therefore, it is conceivable that a greater effect on AKI could be achieved by administering an adequate dosage of amino acids.

Although not statistically significant, subgroup analysis showed a trend in favor of the control group in the order of supra-renal, semi-renal, and infra-renal (Table 4). The hypothesis of this study posited that AKI would be mitigated by an increase in renal blood flow resulting from amino acid administration. However, there are two potential mechanisms underlying AKI following open abdominal aortic aneurysm repair: reduced renal blood flow due to ischemia-reperfusion injury and direct blood flow obstruction caused by supra-renal cross-clamp. The former is also caused by infra-renal cross-clamp, and the chemical mediator-mediated mechanism might be alleviated by the actions of amino acids. The latter, on the other hand, involves a direct blockade of blood flow and may not benefit from amino acid administration.

There was little difference in the minimum body temperature during surgery between the two groups. This result is not unexpected since the amino acids were infused in order to raise body temperature during surgery. Moreover, the result is reasonable because the effect of amino acid infusion on the incidence of AKI is not mediated by body temperature.

This study had several limitations. Firstly, some data were unavailable because of automated extraction from medical records. Therefore, we could not adjust for several factors that might be associated with postoperative outcomes such as aortic cross-clamp time, postoperative fluid balance, intraoperative cardiovascular variables, and preoperative comorbidity. As the duration of blood flow cessation to the renal artery during suprarenal cross-clamping is particularly important, the location of aortic cross-clamp was substituted for the duration of blood flow cessation to the renal artery by incorporating the location of aortic cross-clamp within the statistical model. Moreover, there was no data on the intraoperative renal blood flow because the data was not measured in regular medical care. Therefore, it could not be concluded that amino acids suppressed the AKI by increasing the renal blood flow.

Secondly, the study enrollment period was approximately 12 years. Since surgical procedures have changed over 12 years, such as the transition from open surgery to endovascular surgery, the characteristics of patients who undergo open surgery might also have changed. To address this issue, our statistical analysis included adjustments for the year of surgery.

Lastly, the criteria for the infusion of amino acids by the attending anesthetist are not clear. However, the anesthetists infused it to maintain body temperature but not for AKI prophylaxis. Furthermore, body temperatures were similar between the two groups. Therefore, we believe this factor doesn't significantly introduce bias into our analysis.

In conclusion, we could not show the effect of intraoperative amino acid infusion on AKI after open AAA repair. In our study, the dosage of amino acids administrated was considerably less than that in previous studies. Therefore, it is possible that an adequate dosage of amino acids may have an effect on AKI, and further studies are needed.

Acknowledgements

All authors have no COI to declare regarding the present study.

We would like to thank Mr. Bito, Dr. Minami and Dr. Yoshitani for their valuable contributions to this study.

References

1. Brinkman R, HayGlass KT, Mutch WA, et al. Acute kidney injury in patients undergoing open abdominal aortic aneurysm repair: a pilot observational trial. J Cardiothorac Vasc Anesth 2015;29:1212-1219.
2. Castagno C, Varetto G, Quaglino S, et al. Acute kidney injury after open and endovascular elective repair for infrarenal abdominal aortic aneurysms. J Vasc Surg 2016;64:928-933.
3. Dubois L, Durant C, Harrington DM, et al. Technical factors are strongest predictors of postoperative renal dysfunction after open transperitoneal juxtarenal abdominal aortic aneurysm repair. J Vasc Surg 2013;57:648-654.
4. Hoshina K, Nemoto M, Shigematsu K, et al. Effect of suprarenal aortic cross-clamping. Circ J 2014;78:2219-2224.
5. Shahverdyan R, Majd MP, Thul R, et al. F-EVAR does not impair renal function more than open surgery for juxtarenal aortic aneurysms: single centre results. Eur J Vasc Endovasc Surg 2015;50:432-441.
6. Tallgren M, Niemi T, Pöyhiä R, et al. Acute renal injury and dysfunction following elective abdominal aortic surgery. Eur J Vasc Endovasc Surg 2007;33:550-555.
7. Kheterpal S, Tremper KK, Heung M, et al. Development and validation of an acute kidney injury risk index for patients undergoing general surgery: results from a national data set. Anesthesiology 2009;110:505-515.
8. Chew STH, Hwang NC. Acute kidney injury after cardiac surgery: a narrative review of the literature. J Cardiothorac Vasc Anesth 2019;33:1122-1138.
9. Brezis M, Silva P, Epstein FH. Amino acids induce renal vasodilatation in isolated perfused kidney: coupling to oxidative metabolism. Am J Physiol 1984;247:H999-1004.
10. Fliser D, Zeier M, Nowack R, et al. Renal functional reserve in healthy elderly subjects. J Am Soc Nephrol 1993;3:1371-1377.
11. Sharma A, Zaragoza JJ, Villa G, et al. Optimizing a kidney stress test to evaluate renal functional reserve. Clin Nephrol 2016;86:18-26.
12. Woods LL. Mechanisms of renal hemodynamic regulation in response to protein feeding. Kidney Int 1993;44:659-675.
13. Chen C, Mitchell KD, Navar LG. Role of endothelium-derived nitric oxide in the renal hemodynamic response to amino acid infusion. Am J Physiol Regul Integr Comp Physiol 1992;263:R510-R516.
14. Yeung KK, Groeneveld M, Lu JJ, et al. Organ protection during aortic cross-clamping. Best Pract Res Clin Anaesthesiol 2016;30:305-315.
15. JCS Joint Working Group. Guidelines for diagnosis and treatment of aortic aneurysm and aortic dissection (JCS 2011). Circ J 2013;77:789-828.
16. Khwaja A. Kdigo clinical practice guidelines for acute kidney injury. Nephron Clin Pract 2012;120:c179-184.
17. Little R, An H. Robust likelihood-based analysis of multivariate data with missing values. Stat Sin 2004;14:949-968.
18. Pu H, Doig GS, Heighes PT, et al. Intravenous amino acid therapy for kidney protection in cardiac surgery patients: a pilot randomized controlled trial. J Thorac Cardiovasc Surg 2019;157:2356-2366.
19. Giordano M, Castellino P, McConnell EL, et al. Effect of amino acid infusion on renal hemodynamics in humans: a dose-response study. Am J Physiol 1994;267:F703-F708.

Osaka City Med. J. Vol. 70, 19-25, 2024

Multiple Cerebral Infarctions due to a Calcified Amorphous Tumor that was Surgically Resected Successfully: A Case Report

Kosuke Okamoto[1)], Mayu Shiomi[1)], Keisuke Togawa[1)], Hiroka Sakaguchi[1)], Akitoshi Takeda[1)], Takenobu Shimada[2)], Akimasa Morisaki[3)], Yuko Kuwae[4)], Masahiko Ohsawa[4)], and Yoshiaki Itoh[1)]

Departments of Neurology[1)], Cardiology[2)], Cardiosurgery[3)], and Pathology[4)], Graduate School of Medicine, Osaka Metropolitan University

Abstract

Calcified amorphous tumor (CAT) is a recently recognized non-neoplastic cardiac tumor; however, its clinical relevance remains unclear. We report a case of a patient with CAT who suddenly developed motor aphasia. Head magnetic resonance imaging revealed multiple small cerebral infarctions in the scattered cerebral cortices. Transesophageal echocardiography and chest computed tomography revealed a 2-cm mass attached to the posterior mitral leaflet. The patient was diagnosed with CAT-induced infarction and was successfully treated with surgery. As antithrombotic treatment for CAT has not been effective in preventing infarction in most previous reports, prompt surgical resection is recommended.

Key Words: Cardioembolism; Type 2 diabetes, Posterior mitral leaflet; Non-neoplastic tumor; Transesophageal echocardiography

Introduction

Calcified amorphous tumor (CAT) is a non-neoplastic tumor first reported by Reynolds et al in 1997[1)]. It histologically consists of calcified nodules with amorphous materials and is commonly detected incidentally in cardiac imaging studies. However, the clinical association between CAT and cerebral infarction remains unclear[2)]. Herein, we report a case of CAT with multiple scattered cerebral embolic infarctions that was surgically resected.

Case Report

A 69-year-old Japanese man suddenly noticed difficulty in choosing words during lunch with his family at 1200 hours. He visited a nearby clinic and underwent emergency brain magnetic resonance imaging (MRI) that revealed multiple infarctions in the acute and subacute phases. The patient was transferred to our hospital at 1700 hours. He had been diagnosed with type 2 diabetes for 10 years and was being treated with metformin. He had smoked 20 cigarettes per day for the past 50 years.

Received May 1, 2023; accepted June 13, 2023.
Correspondence to: Yoshiaki Itoh, MD.
Department of Neurology, Graduate School of Medicine, Osaka Metropolitan University,
1-4-3 Asahimachi, Abeno-ku, Osaka 545-8585, Japan
Tel: +81-6-6645-3889; Fax: +81-6-6646-5599
E-mail: y-itoh@omu.ac.jp

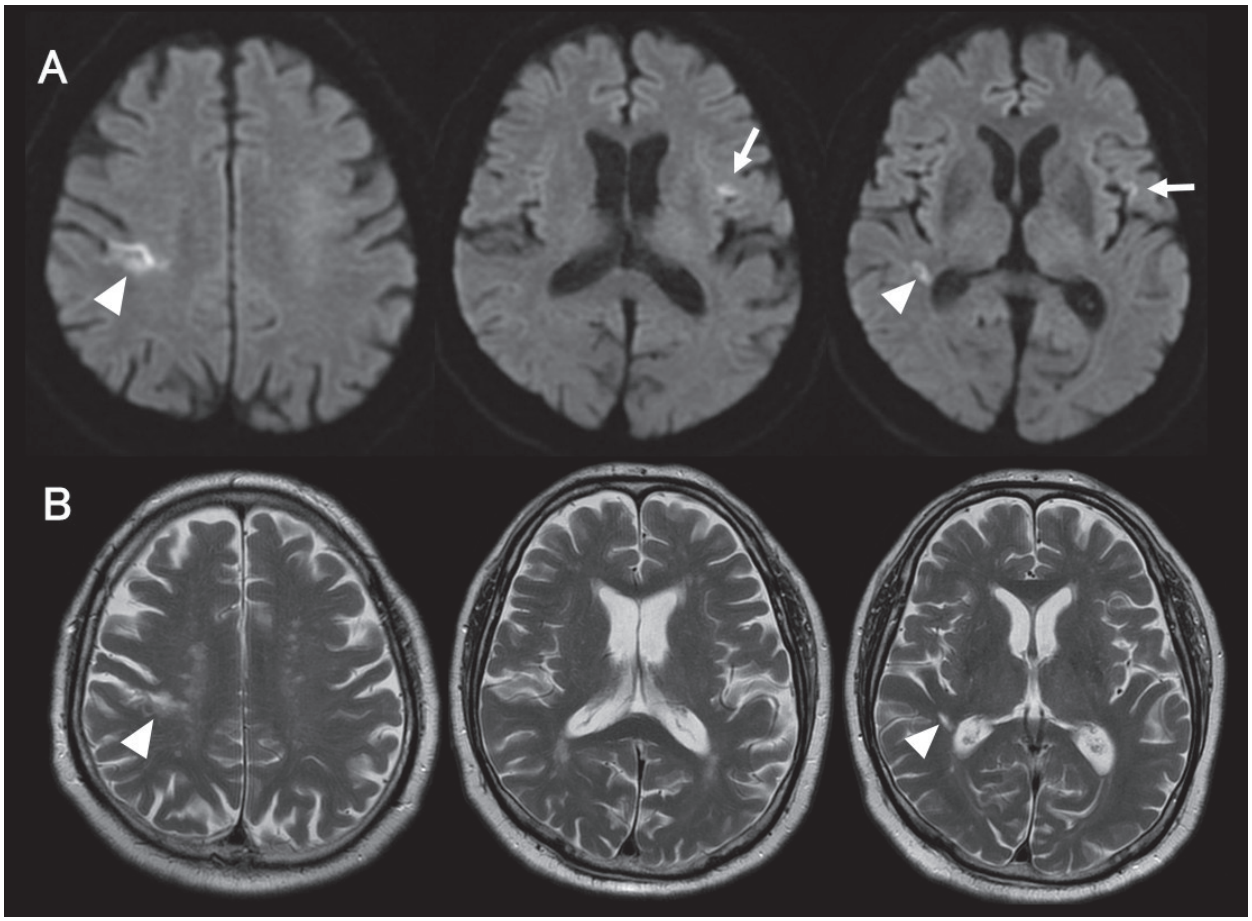

Figure 1. Brain magnetic resonance imaging (MRI) images taken on day 1. Diffusion-weighted MRI images (arrow, A) demonstrate a small infarct with a 5-mm diameter in the left insular cortex. The lesion was not detected on T2-weighted images (B), suggesting an acute lesion. A small infarct in the subacute phase was observed in the precentral gyrus and another in the deep white matter below the cortical one on the right side on diffusion-weighted (arrow head, A) and T2-weighted images (arrow head, B).

He had no family history of stroke or any specific cardiac diseases.

On admission, his height was 168 cm, weight was 82.4 kg, body mass index was 28.9, blood pressure was 140/80 mm Hg, and pulse rate was 69/min and regular. Physical examination revealed no carotid bruit on either side and no cardiac murmurs. Neurological examination revealed that the patient was right-handed. He was conscious and alert. However, his spontaneous speech was not fluent. He had difficulty naming objects and paraphasia. He was unable to repeat long sentences, although his understanding of spoken words was preserved. He had neither cranial nerve abnormalities nor weakness. His deep tendon reflexes were normal. All pathological reflexes were negative. The patient's sensory system was normal. The coordination tests revealed no abnormalities. His station and gait were stable. His National Institutes of Health Stroke Scale (NIHSS) score[3] was 1.

Laboratory tests revealed the following results: WBC 6700/μL; RBC 327×10^4/μL; hemoglobin 15.4 g/dL; platelet count, 26.3×10^4/μL; D-dimer <0.5 μg/mL; BUN 15 mg/dL; Cr 0.89 mg/dL; LDL 125 mg/dL; plasma glucose, 130 mg/dL; HbA1c 8.7%; Ca 9.3 mg/dL; P 3.3 mg/dL, and BNP 13.5 pg/mL. Twelve-lead electrocardiography revealed a normal sinus rhythm of 61 beats/min.

Diffusion-weighted MRI revealed a small infarct with a diameter of 5 mm in the left insular cortex (Fig. 1A). The lesion was not detected on Fluid Attenuated Inversion Recovery (FLAIR) images and

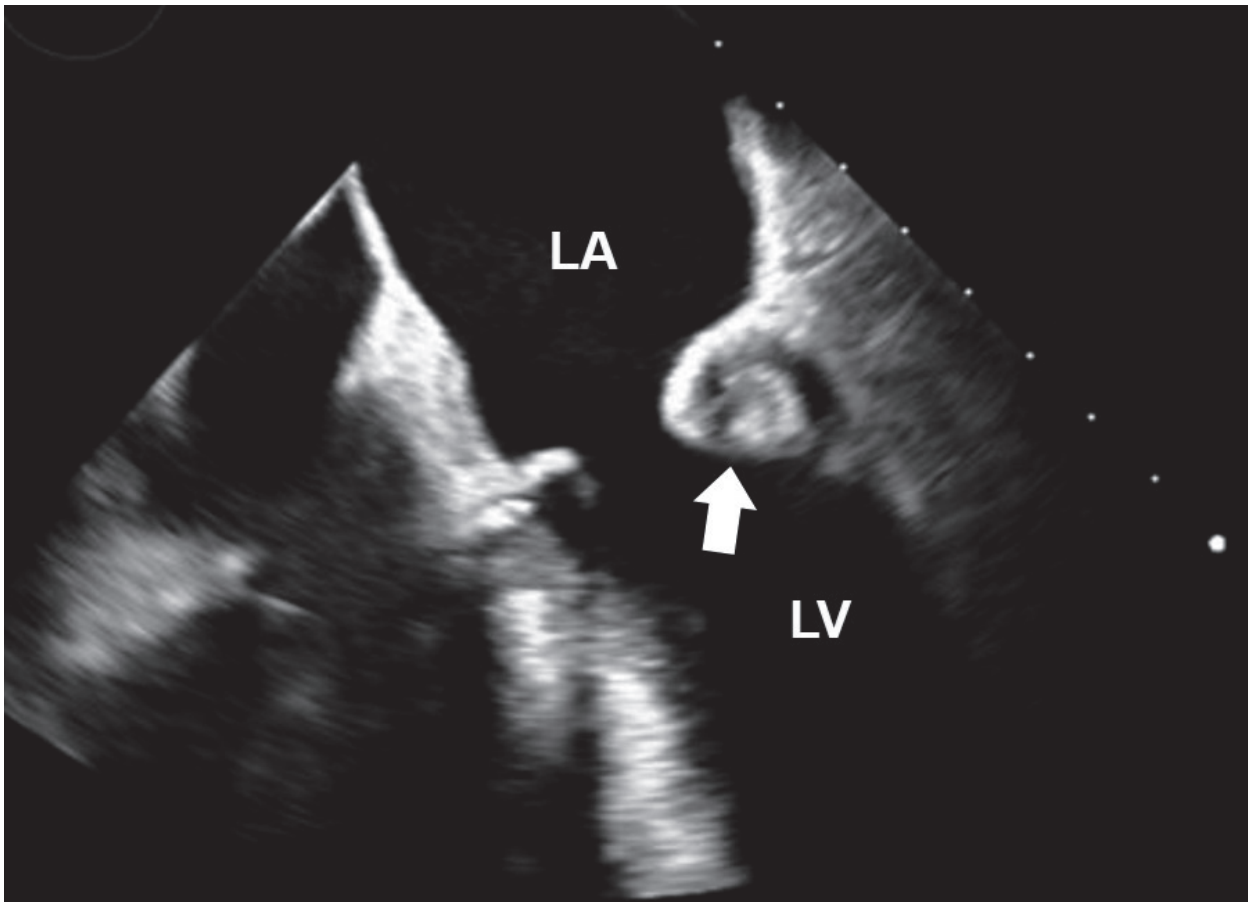

Figure 2. Transesophageal echocardiography revealed a mass with a 2-cm diameter attached to the posterior mitral leaflet (arrow). The contents of the tumor were heterogeneously visualized. LA, left atrium; LV, left ventricle.

T2-weighted images, suggesting an acute lesion (Fig. 1B). Additionally, small infarcts in the subacute phase were identified in the precentral gyrus and deep white matter adjacent to the cortical lesion on the right side on diffusion-weighted and T2-weighted images. Magnetic Resonance angiography revealed no abnormalities in the major cerebral arteries.

Based on the time window and MRI findings, the patient was not considered for intravenous thrombolysis or mechanical thrombectomy. He was started on dual antiplatelet therapy with aspirin (100 mg once daily) and clopidogrel (75 mg once daily), as well as intravenous argatroban (60 mg over 24hours for 2 days followed by 10 mg twice daily for 5 days) and edaravone (30 mg twice daily for 14 days).

Holter electrocardiographic monitoring revealed no arrhythmia. Transthoracic echocardiography revealed a mass around the posterior mitral leaflet. Transesophageal echocardiography revealed a tumor of 2-cm diameter attached to the posterior mitral leaflet (Fig. 2). The tumor contents were heterogeneously visualized. No intracardiac thrombus was observed. Echocardiography revealed no significant atherosclerotic plaques in the aorta or the patent foramen ovale. Chest computed tomography (CT) revealed a heterogeneously calcified mass of 2 cm in diameter, part of which was enhanced with contrast medium (Fig. 3). Carotid ultrasonography revealed small plaques without significant stenosis or an increase in flow velocity on both sides. Leg ultrasonography revealed no deep venous thrombosis.

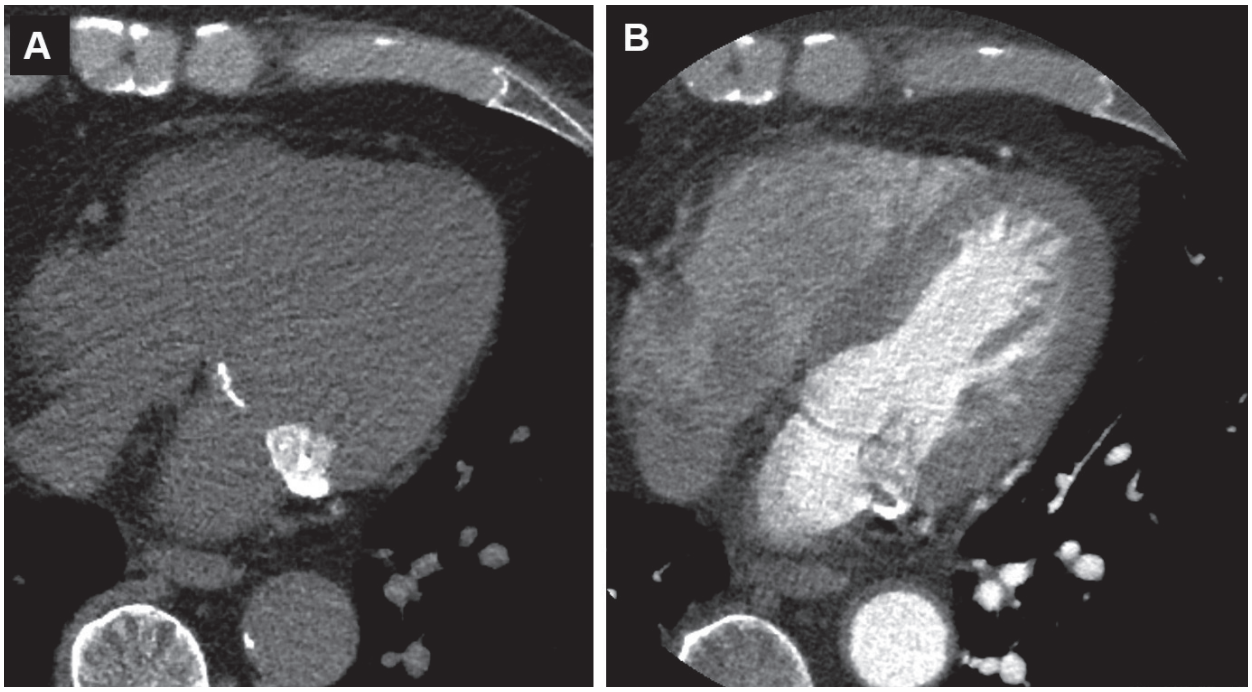

Figure 3. Plain chest computed tomography revealed a heterogeneously calcified mass with a 2-cm diameter (A), part of which was enhanced with contrast medium (B).

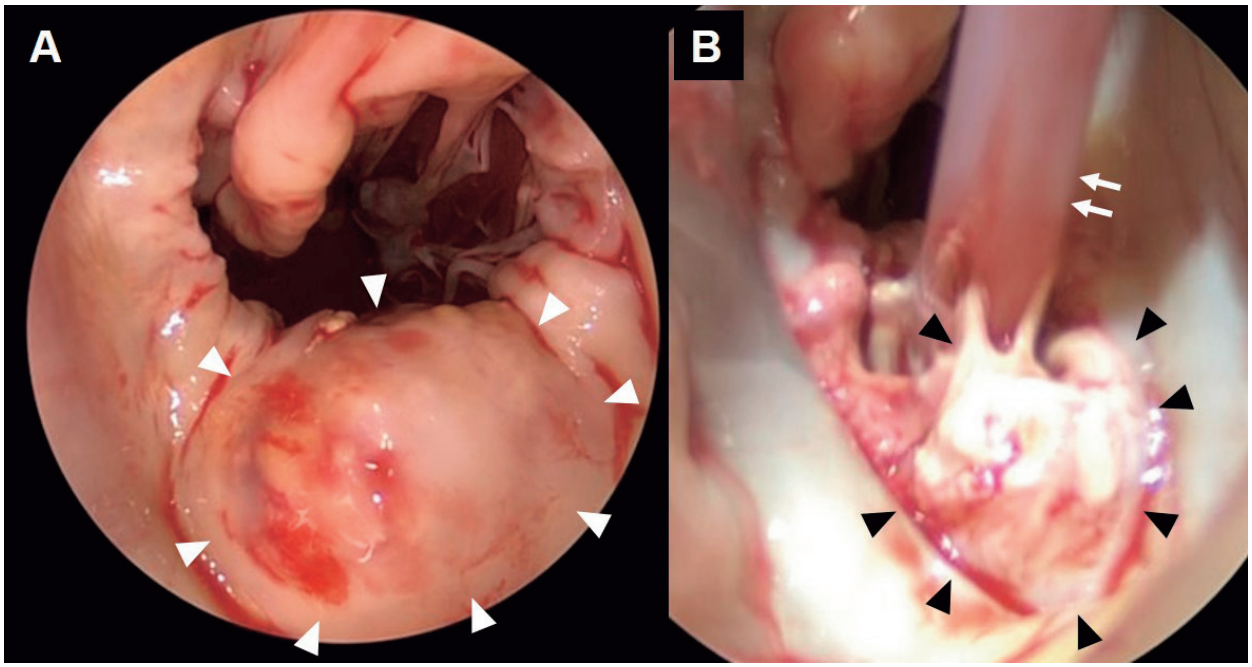

Figure 4. Intraoperative findings. A round elevated mass with a 2-cm diameter was located on the mitral annulus and extending to the posterior mitral leaflet (arrow head, A). Its surface was ulcerated, and calcified material was observed underneath. Upon resection of the posterior mitral leaflet, a creamy white discharge, consistent with caseous calcification, appeared (arrow head, B). The amorphous material was aspirated with a suction (arrow, B).

The patient was diagnosed with multiple CAT-induced infarctions and was at a high risk of recurrent infarction. On day 15, the patient underwent surgical resection of the intracardiac tumor. Intraoperative findings revealed a round elevated mass of 2-cm diameter located on the mitral

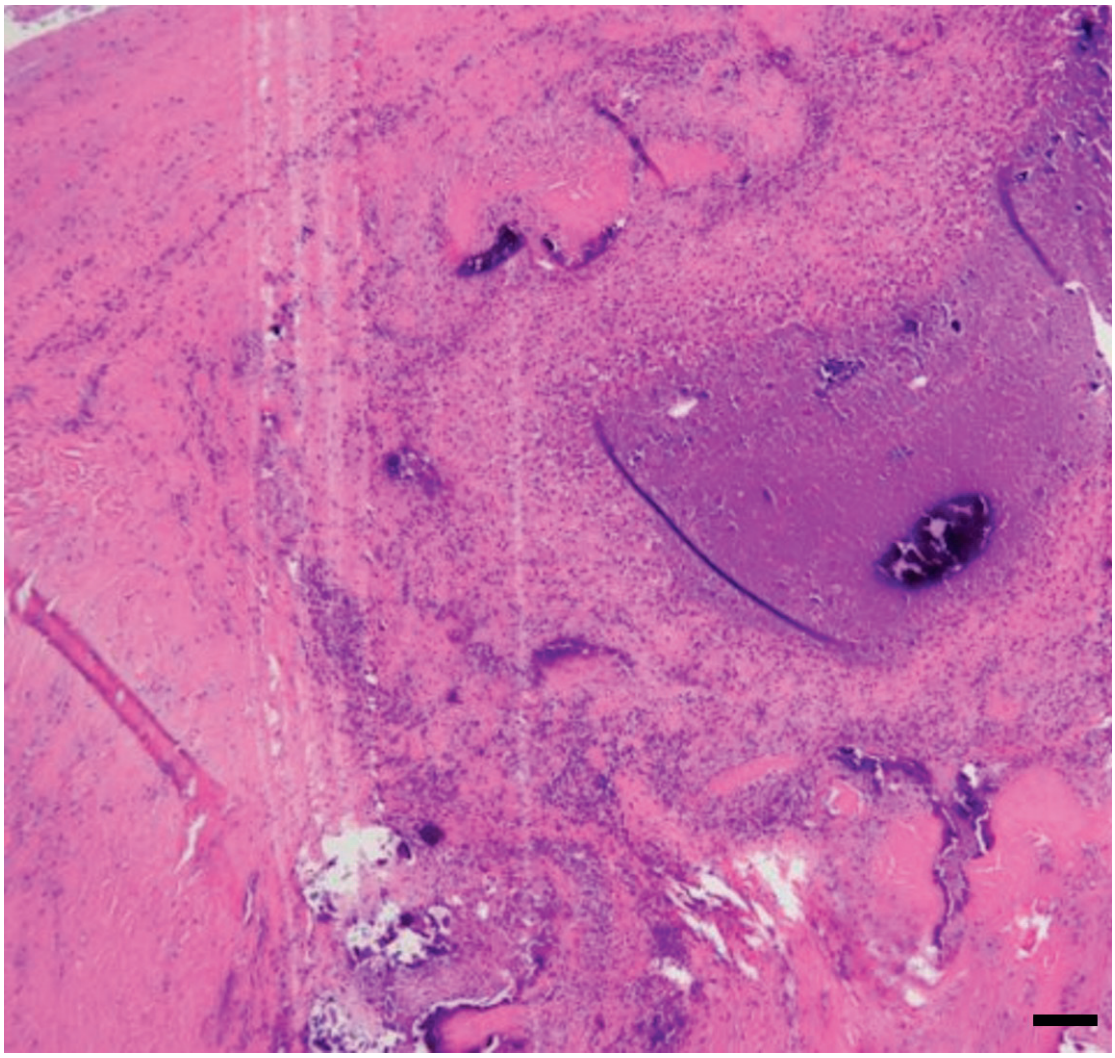

Figure 5. Pathological findings. Nodular calcification deposits are observed adjacent to the creamy amorphous material, which is surrounded by infiltrated inflammatory cells. The surface of the lesion is coated with fibrin. Scale: 100 µm.

annulus and extending to the posterior mitral leaflet (Fig. 4A). Its surface was ulcerated, and calcified material was observed underneath. Upon resection of the posterior mitral leaflet, a creamy white discharge consistent with caseous calcification appeared (Fig. 4B). The amorphous material was aspirated with a suction. The mitral annulus was reconstructed with a bovine pericardial patch and the mitral valves were replaced with bioprosthetic valves (Mosaic Bioprosthesis, Medtronic Japan Co., LTD, Tokyo, Japan).

Pathological examination revealed nodular calcification deposits adjacent to the creamy amorphous material surrounded by infiltrated inflammatory cells (Fig. 5). The lesion surface was coated with fibrin. These pathological findings were consistent with typical CAT pathology reported previously[1,2].

The dual antiplatelet therapy was terminated after the surgery. Aphasia, the only neurological symptom, quickly disappeared after admission, and the patient's recovery from the surgery was good. The patient was discharged on day 29 without any residual symptoms and had no recurrent attacks for 2 years.

Discussion

CAT was first reported as a non-neoplastic intracardiac tumor in 1997[1]. Pathologically, the lesion comprises nodular deposits or flecks of calcium with eosinophilic, amorphous, and occasionally fibrillar material. Although the nature of the amorphous material is unclear, it is suggestive of fibrin degeneration. Nodular calcium deposits are intervened with the dense collagen and chronic inflammatory cells. Most patients have fresh fibrin on the surfaces of the tumor, and the tumor is anchored to the subjacent endomyocardium by either dense connective tissue or granulation tissue associated with chronic inflammation. These characteristics are consistent with the pathological findings in the present case.

Pathological differential diagnoses include most benign and malignant cardiac tumors, predominantly myxoma and non-neoplastic processes, including thrombus, embolus, and vegetation[4]. The infiltration of inflammatory cells observed in the present case was non-specific and mild and was not suggestive of endocarditis as a primary cause of the lesion. A similar inflammatory change was observed in all 11 cases in the first report of CAT[1]. Mitral annular calcification, a non-inflammatory chronic degenerative process of the fibrous support structure of the mitral valve[5], does not include amorphous material and inflammatory changes and is distinct from CAT. CAT is often accompanied by mitral annular calcification[2]. In the present case, although the calcified lesion was adhered to the mitral annulus ring, the pathological changes were specific to CAT, and no additional lesions suggestive of mitral annular calcification were observed.

Most CAT cases present with cardiac symptoms, including chest pain, syncope, and shortness of breath. Cerebral infarction was reported in 2 of 11 cases (18%) in the first CAT report[1] and in 16 of 83 cases (19%) in a recent review[6]. Furthermore, in a review of 18 CAT-induced cerebral infarction cases, 9 cases (50%) had multiple lesions[2]. These lesions were mostly small or punctate, as in the present case. Correspondingly, neurological symptoms at onset were generally mild (NIHSS 2-4 points), and the prognosis was favorable, as observed in the present case[6]. The small size of the infarction on CT or MRI and mild symptoms suggest that small emboli may occlude the cerebral arteries in CAT-induced infarctions. Based on the pathological findings of CAT indicating an ulcerated surface, fragments of the fibrin cap or scattering of amorphous material detached or released from the CAT may occlude multiple arteries[7].

The risk factors for CAT include end-stage renal disease, diabetes mellitus, and hypertension[8]. Although the detailed etiology of CAT remains unclear, abnormal calcium metabolism and chronic inflammation associated with these risk factors may induce CAT. Additionally, CAT accompanied by mitral annular calcification may be associated with an atherosclerotic process[9]. The patient in the current report had poorly controlled type 2 diabetes, obesity, and smoking as risk factors. Although a few cases of infectious endocarditis-associated CAT were reported recently[10-13], it may be considered a distinct entity.

Surgical resection is typically selected to prevent cerebral infarction and for pathological confirmation[2]. Meanwhile, the efficacy of antithrombotic drugs has not yet been fully evaluated. In the present case, prompt surgical resection after admission prevented further recurrence for 2 years.

In conclusion, we report a rare case of CAT with multiple scattered cerebral embolic infarctions. Scrupulous evaluation of the heart and prompt resection of the lesion once suspected of CAT is recommended.

Acknowledgements

All authors have no COI to declare regarding the present study.

References

1. Reynolds C, Tazelaar HD, Edwards WD. Calcified amorphous tumor of the heart (cardiac CAT). Hum Pathol 1997;28:601-606.
2. Nishiguchi Y, Matsuyama H, Shindo A, et al. Cerebral embolism associated with calcified amorphous tumor: a review of cerebral infarction cases. Intern Med 2021;60:2315-2319.
3. Brott T, Adams HP Jr, Olinger CP, et al. Measurements of acute cerebral infarction: a clinical examination scale. Stroke 1989;20:864-870.
4. Pietro DA, Parisi AF. Intracardiac masses. Tumors, vegetations, thrombi, and foreign bodies. Med Clin North Am 1980;64:239-251.
5. Benjamin EJ, Plehn JF, D'Agostino RB, et al. Mitral annular calcification and the risk of stroke in an elderly cohort. N Engl J Med 1992;327:374-379.
6. Takahashi Y, Niino T. Cardiac calcified amorphous tumor presenting as cerebral infarction. Japanese Journal of Cardiovascular Surgery 2020;49:16-20. (In Japanese)
7. Greaney L, Chaubey S, Pomplun S, et al. Calcified amorphous tumour of the heart: presentation of a rare case operated using minimal access cardiac surgery. BMJ Case Rep 2011;2011:bcr0220113882.
8. Ogasawara Y, Mano K, Henmi F, et al. A case of caseous calcification of mitral annulus resulting in multiple cerebral infarctions. Rinsho Shinkeigaku 2023;63:97-100. (In Japanese)
9. Ushioda R, Shirasaka T, Kikuchi S, et al. Calcified amorphous tumor located on a severely calcified mitral annulus in a patient with normal renal function. J Surg Case Rep 2022;2022:rjab608.
10. Kimura M, Niwa JI, Ito H, et al. Multiple cerebral infarctions due to calcified amorphous tumor growing rapidly from an antecedent infection and decreasing rapidly by detachment of fibrin and antithrombotic drugs: a case report. BMC Neurol 2022;22:391.
11. Koito S, Unoki Y, Yoshida K, et al. Importance of early diagnosis and surgical treatment of calcified amorphous tumor-related native valve endocarditis caused by Escherichia coli: a case report. BMC Infect Dis 2022;22:226.
12. Handa K, Fukui S, Shirakawa Y, et al. Infective calcified amorphous tumor on mitral valve and critical course of left ventricular rupture. J Cardiol Cases 2021;24:182-185.
13. Okazaki A, Oyama Y, Hosokawa N, et al. The first report of calcified amorphous tumor associated with infective endocarditis: a case report and review of literature. Am J Case Rep 2020;21:e922960.

Osaka City Med. J. Vol. 70, 27-34, 2024

Jejunal Herniation into the Lesser Sac through a Defect in the Gastrocolic Ligament Diagnosed with Multidetector Computed Tomography: A Case Report

Noriko Takeshita[1], Kiyotaka Yukimoto[2], Masahiro Tokunaga[1], Tomohiro Ohira[1], Hiroyuki Maeda[3], and Tohru Takeshita[4]

Departments of Radiology[1] and Surgery[2], Izumi City General Hospital;
Department of Diagnostic and Interventional Radiology[3],
Graduate School of Medicine, Osaka Metropolitan University; and
Department of Radiology[4], Osaka Habikino Medical Center

Abstract

Internal hernia (IH) into the lesser sac through a defect in the gastrocolic ligament (GCL) of the greater omentum, an emergency abdominal condition, is a type of IH that involves the greater omentum. Because its clinical symptoms are non-specific, so clinically its preoperative diagnosis is usually difficult. Here, we report a case of IH into the lesser sac through a defect in the GCL in which multi-detector computed tomography (MDCT) clearly showed penetration of the jejunum with its mesenteric fat tissue and mesenteric vessels through a complete defect in the GCL. These MDCT findings accurately reflected the direct findings of this rare type of IH, so we were confident in the preoperative diagnosis.

Key Words: Internal hernia; Omentum; Gastrocolic ligament; Lesser sac; Multidetector computed tomography

Introduction

Internal hernia (IH) involving the greater omentum can be classified into three types[1-11]. Herniation of viscus through a defect in the free-hanging part of the greater omentum is the most common IH type, which has been historically referred to as trans-omental hernia. This type involves the small bowel in almost all cases[1-4], and the herniated small bowel without a hernia sac lies in the inframesocolic compartment of the greater peritoneal cavity. The second IH type is herniation of the small bowel into the lesser sac through a defect in the gastrocolic ligament (GCL)[5,6], and the herniated small bowel is trapped within the lesser sac. The third IH type is a special presentation of the second type[7-11]. The herniated small bowel, which has entered into the lesser sac from a defect in the GCL, re-enters the greater peritoneal cavity from a defect in the lesser omentum or the foramen of Winslow. Sometimes, IH traversing the lesser sac from defects in both the GCL and the lesser omentum is

Received May 31, 2023; accepted November 28, 2023.
Correspondence to: Noriko Takeshita, MD.
Department of Radiology, Izumi City General Hospital,
4-5-1 Wake-cho, Izumi City, Osaka 594-0073, Japan
Tel: +81-725-41-1331; Fax: +81-725-43-3350
E-mail: nrktnk1026@gmail.com

termed as double omental hernia[10,11].

A typical patient with IH involving the greater omentum is a middle-aged male or female with no history of abdominal surgery who presents with symptoms such as abdominal pain, abdominal distension, nausea, and vomiting[1-11]. Clinical diagnosis is generally difficult because of non-specific clinical symptoms[1-11]. Therefore, imaging studies play an important role in diagnosis. Currently, multidetector computed tomography (MDCT) is the most used imaging modality for preoperative imaging diagnosis of various IH types[2,3]. However, to our knowledge, no study to date provided detailed MDCT findings of IH entering the lesser sac through a defect in the GCL. Here, we report

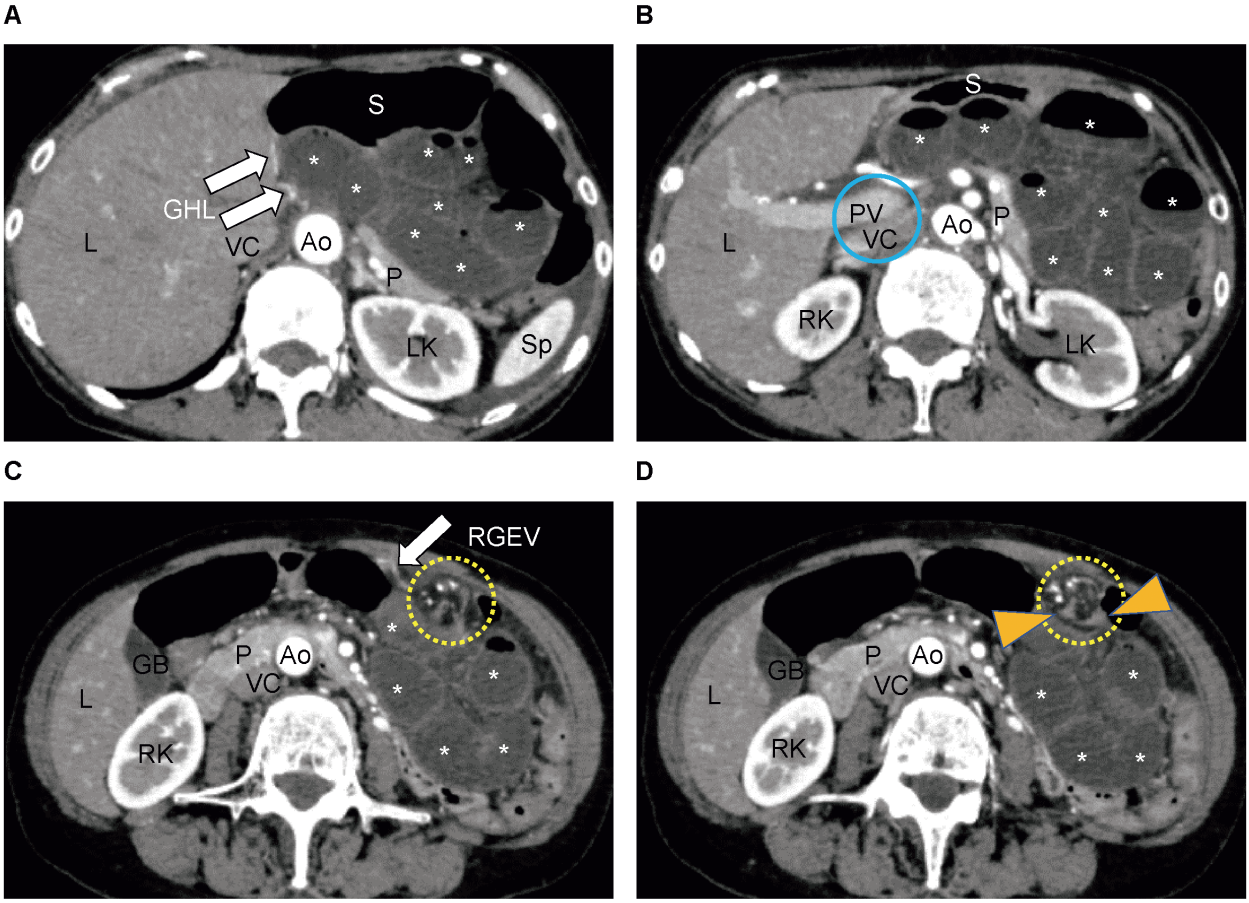

Figure 1. (A-D) Contrast-enhanced axial multidetector computed tomography (MDCT) images from the cephalad (A) to the caudal (D) side.
A: Contrast-enhanced axial MDCT image at the level of the gastrohepatic ligament (a part of the lesser omentum). Herniated jejunal loops (white asterisks) are located in the lesser sac. The stomach body is displaced anteriorly and superiorly. The gastrohepatic ligament (one part of the lesser omentum) is also compressed and stretched.
B: Contrast-enhanced axial MDCT image at the level of the foramen of Winslow. Herniated jejunal loops (white asterisks) are located in the lesser sac. Note that the area at the foramen of Winslow (blue circle) appears normal.
C: Contrast-enhanced axial MDCT image at the level of the caudal part of the stomach body. Herniated jejunal loops (white asterisks) are located in the lesser sac. Note that herniated jejunal vessels and mesenteric fat tissue (yellow dotted circle) are intersecting the gastroepiploic vessels and converging toward the level just below the greater curvature of the stomach.
D: Contrast-enhanced axial MDCT image at the level 4 mm caudal to C. Herniated jejunal loops (white asterisks) are located in the lesser sac. Note that proximal and distal transitional points (orange arrowheads) are adjacent to each another at the level just below the greater curvature of the stomach.
Ao, abdominal aorta; GB, gallbladder; GHL, gastrohepatic ligament; L, liver; LK, left kidney; P, pancreas; PV, portal vein; RGEV, right gastroepiploic vessels; RK, right kidney; S, stomach body; Sp, spleen; and VC, inferior vena cava.

the case of a patient with jejunal herniation into the lesser sac through a defect in the GCL. In this patient, the preoperative diagnosis was based on MDCT findings, which were confirmed by surgery.

Case Report

A 72-year-old woman presented to our hospital with sudden onset of abdominal pain and repeated vomiting starting 20 minutes after a meal. She was in good health except for history of rheumatoid arthritis and cerebral infarction and surgical history of thyroid cancer. Physical examination revealed abdominal distension and epigastric tenderness. No fever was noted. Laboratory tests were within normal limits except for leukocytosis (white blood cell count, 11600/μL; neutrophils, 92.0%). MDCT of the abdomen and pelvis was performed for further investigation. MDCT examination was performed using a 320-detector-row CT scanner (Aquilion ONE; Canon Medical Systems, Otawara,

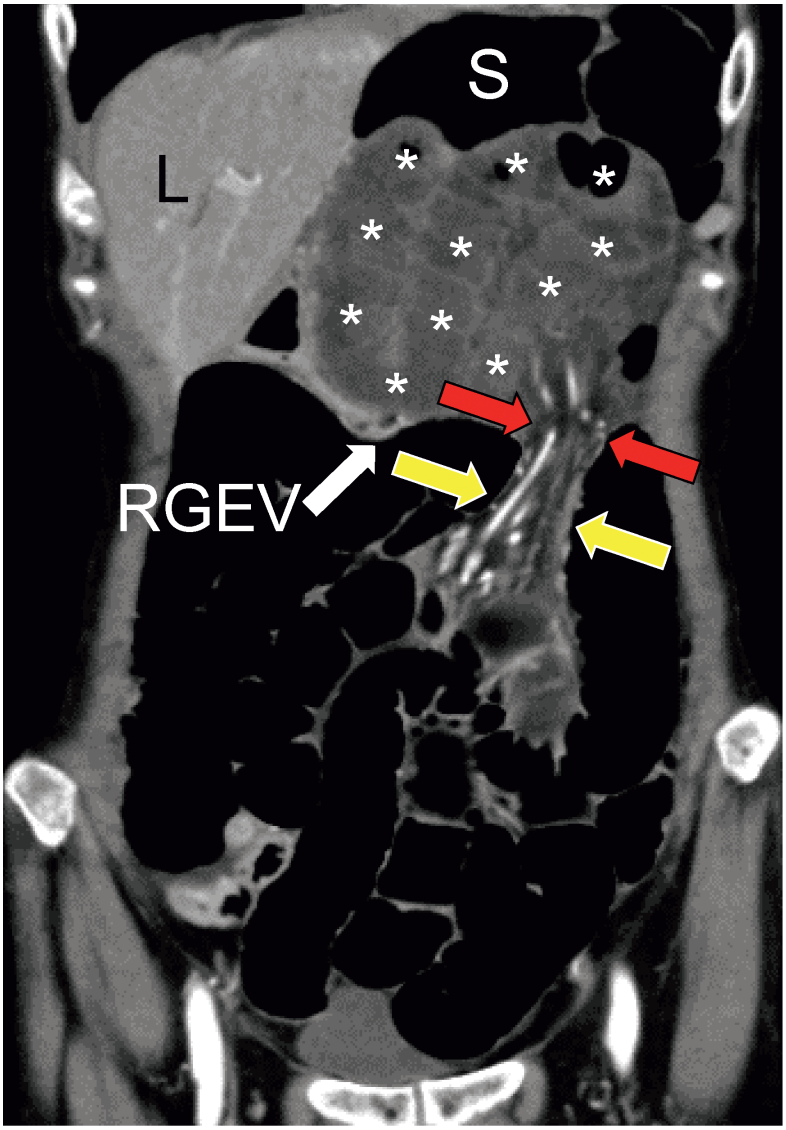

Figure 2. Coronal contrast-enhanced multidetector computed tomography (MDCT) image showing incarcerated jejunum herniating into the lesser sac (white asterisks). Jejunal vascular pedicle (yellow arrows) is running upward and passing through the hernia orifice (red arrows).
L, liver; RGEV, right gastroepiploic vessels; and S, stomach body.

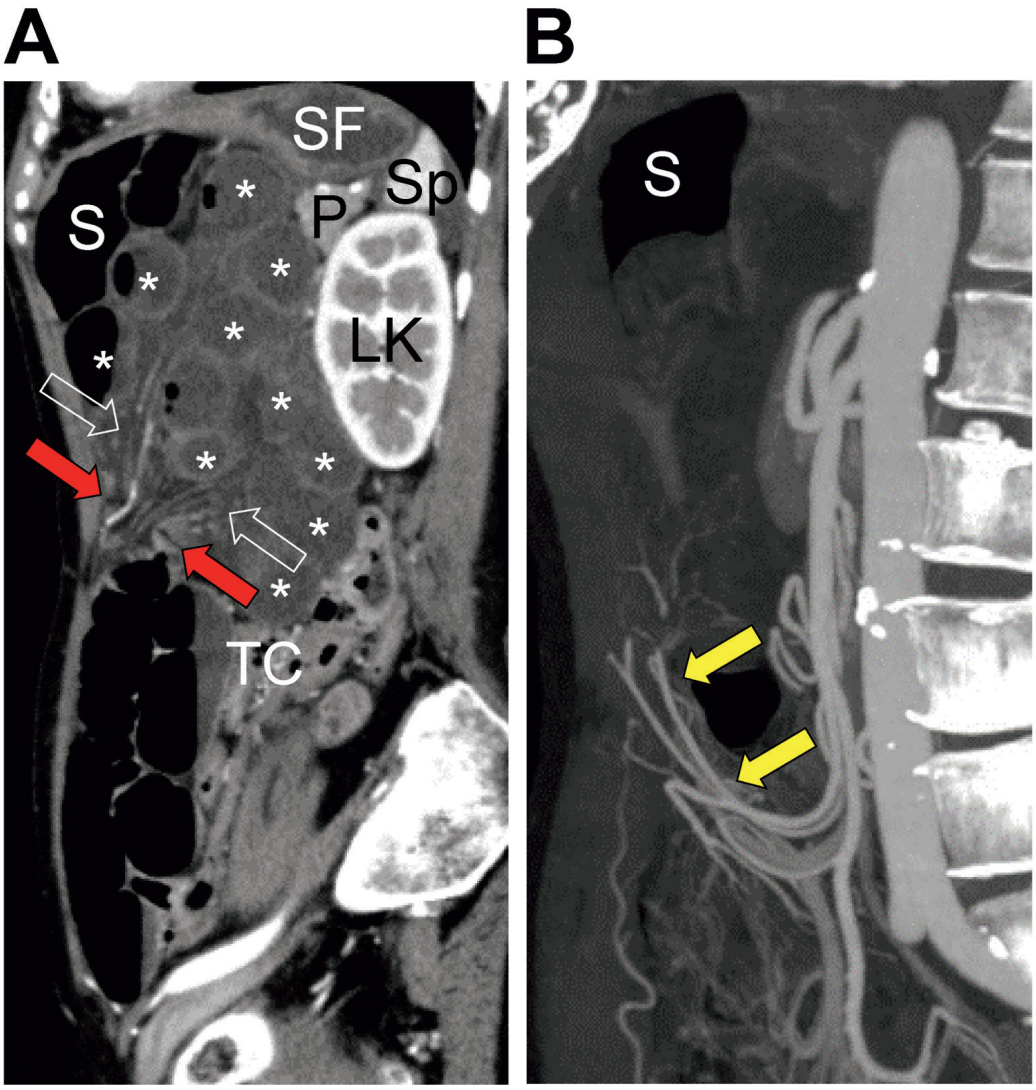

Figure 3. (A) Sagittal contrast-enhanced multidetector computed tomography (MDCT) image showing herniation and incarceration of the jejunum (white asterisks) into the lesser sac. Herniated jejunal vessels and mesenteric fat tissue (transparent arrows) are visualized as radiating forms and converging toward the hernia orifice (red arrows). Note hernia orifice located in the anterocaudal aspect of the lesser sac. (B) Sagittal contrast-enhanced MDCT maximum intensity projection image. Jejunal vessels show an abrupt change in direction (yellow arrows), running upward and finally entering the lesser sac.
LK, left kidney; P, pancreas; S, stomach body; SF, stomach fundus; Sp, spleen; and TC, transverse colon.

Japan). The scan range was from the diaphragmatic dome to the sciatic tubercle. After non-enhanced CT images were obtained, a multiphasic contrast-enhanced CT was performed. A nonionic iodinated contrast agent containing 300 mg of iodine per mL (iohexol, Omnipaque-300; GE HealthCare Pharma Co, Tokyo, Japan) was injected intravenously at a rate of 3.3 mL/sec using an automated injector. Multi-phasic scans included arterial, portal venous, and delayed phases. MDCT (Figs. 1-4) showed a cluster of fluid-filled and dilated small bowel loops surrounded by liver, stomach, spleen, and pancreas; the observed cluster was anatomically located in the lesser sac. The stomach and the lesser omentum were compressed in the ventral and cephalic directions (Figs. 1A, 1B, 2, 3, and 4). The transverse colon was compressed caudally and dorsally (Figs. 3A and 4). The middle portion of the transverse colon was slightly lifted superiorly (Fig. 4). Crowded mesenteric fat tissue and mesenteric

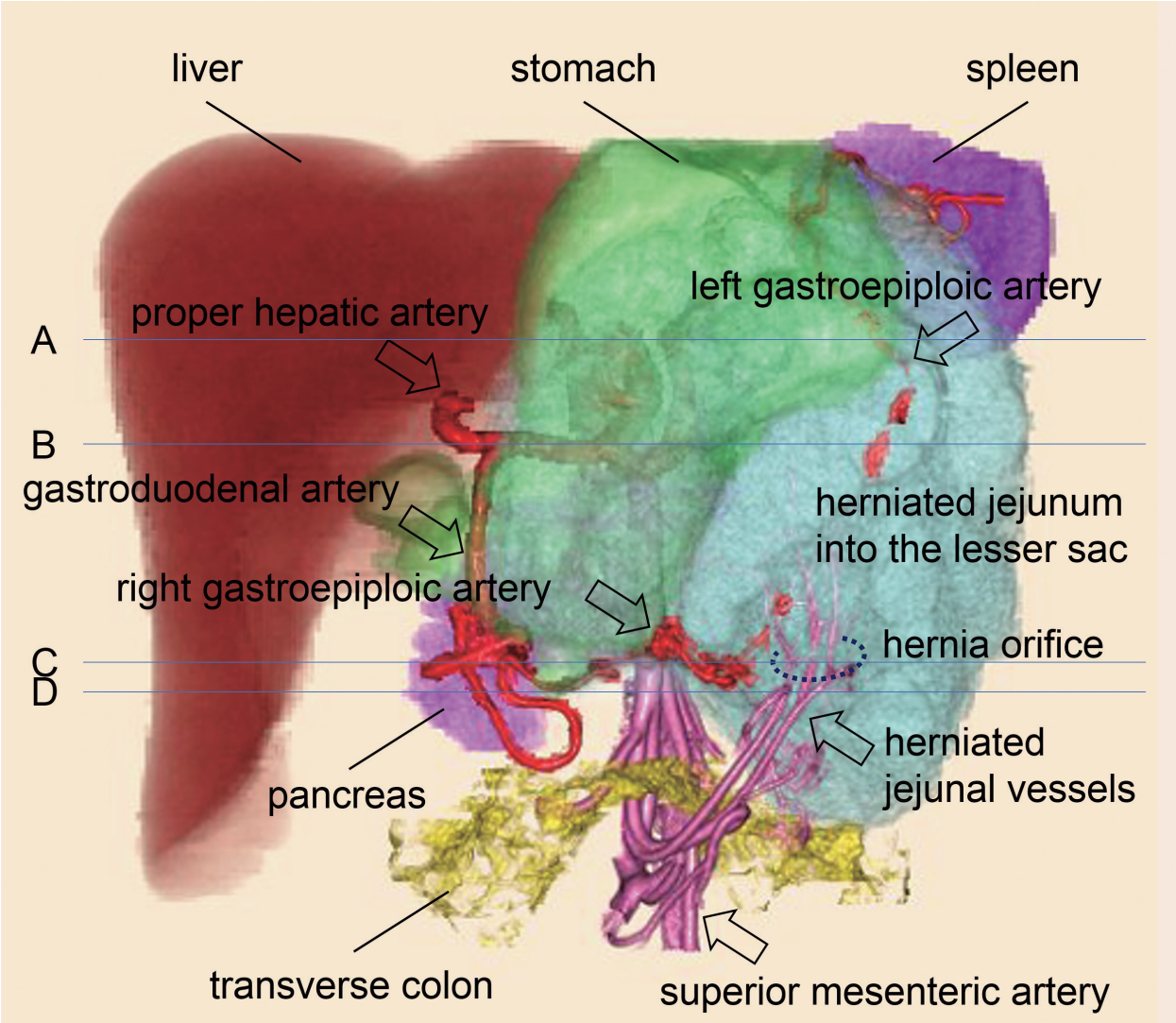

Figure 4. Volume-rendered image showing the well-delineated anatomical relationship of the herniated jejunal loops (light blue) with the surrounding abdominal organs. Note that the herniated jejunal vessels intersect the gastroepiploic vessels and finally enter the lesser sac. Horizontal lines A, B, C, and D correspond to Figures. 1A, 1B, 1C, and 1D of axial contrast-enhanced multi-detector computed tomography (MDCT) images, respectively.

vessels were seen as radiating forms converging caudally at the site of the cluster of fluid-filled and dilated small bowel loops (Figs. 1C, 2, and 3A). At the level just below the greater curvature of the stomach, proximal and distal transitional zones were close to each other (Fig. 1D). The mesenteric fat tissue and mesenteric vessels of the jejunum abruptly turned upward from their normal position and passed between the greater curvature of the stomach and the transverse colon to finally enter the lesser sac (Figs. 2, 3, and 4). The area around the foramen of Winslow was normal (Fig. 1B). A small amount of ascites was observed. Based on these computed tomography (CT) findings, the patient was diagnosed with incarceration of the jejunum herniating into the lesser sac through a defect in the GCL and underwent emergency surgery.

During surgery, a 70-cm-long jejunal loop was found to have herniated through a defect in the GCL to become entrapped in the lesser sac (Fig. 5). The herniated jejunal loops were reduced and repositioned. The initially observed congestion of the herniated jejunal loops and the peristalsis rapidly improved. Thus, bowel resection was not required and the defect in the GCL was closed to

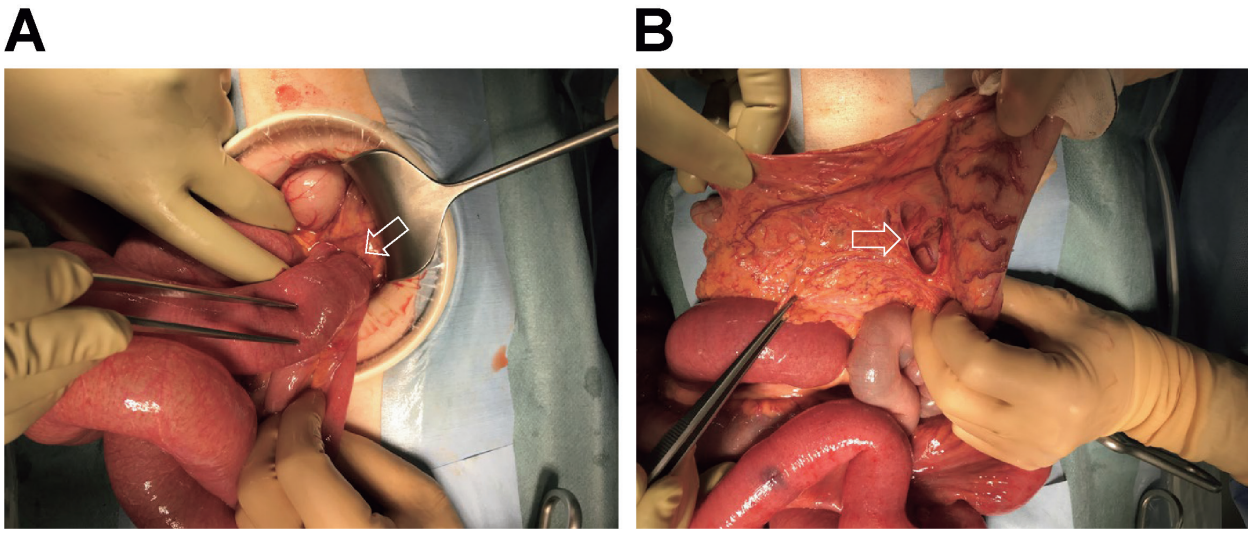

Figure 5. (A, B) Intraoperative photographs. (A) Herniation of the jejunum into the lesser sac from ventral to dorsal through the defect in the gastrocolic ligament (transparent arrow). (B) The defect in the gastrocolic ligament (transparent arrow).

prevent relapse. The postoperative course was uneventful, and the patient was discharged on postoperative day eight. Her subsequent course was uncomplicated.

Discussion

IH is a rare cause of small bowel obstruction, accounting for ≦5.8% of all cases of small bowel obstruction[1]. IH involving the greater omentum accounts for approximately 1%-4% of all IH cases[1]. IH entering the lesser sac through a defect in the GCL is an uncommon type of IH involving the greater omentum[2]. The defect in the GCL can be congenital or acquired[5,6].

Recently, MDCT has become a major modality in the preoperative diagnosis of various types of IHs[2,3]. To the best of our knowledge, detailed MDCT appearance of IH into the lesser sac through a defect in the GCL has not been reported in radiological literature.

The present case illustrates several characteristic CT findings of this IH type. First, the current case was an IH involving jejunal herniation into the lesser sac. The lesser sac is an anatomical potential peritoneal space that communicates with the greater peritoneal cavity through the foramen of Winslow[12]. Normally, the lesser sac is collapsed and empty; it can be recognized posterior to the stomach and anterior to the pancreas on CT[12]. The second characteristic is the abnormal anatomical course of mesenteric fatty tissue and vessels of the herniated jejunum. In the present case, the mesenteric fatty tissue and vessels of the jejunum bent abruptly and ran cephalically, anterior to the transverse colon just below the greater curvature of the stomach, to finally enter the lesser sac. The third characteristic is the site of obstruction, i.e., the hernia orifice through which the small bowel enters the lesser sac. The mesenteric fatty tissue and vessels of the herniated jejunum taper and converge akin a bird's beak toward the caudal side of the greater curvature of the stomach. In the present case, the GCL was this site of convergence and the hernia orifice. On CT, gastroepiploic vessels are the anatomical landmarks for the greater curvature of the stomach and the GCL[12]. In the present case (Fig. 6), combined coronal and sagittal MDCT images and the volume-rendered image allowed the clear visualization of the herniation of the jejunum with the mesenteric fat tissue and

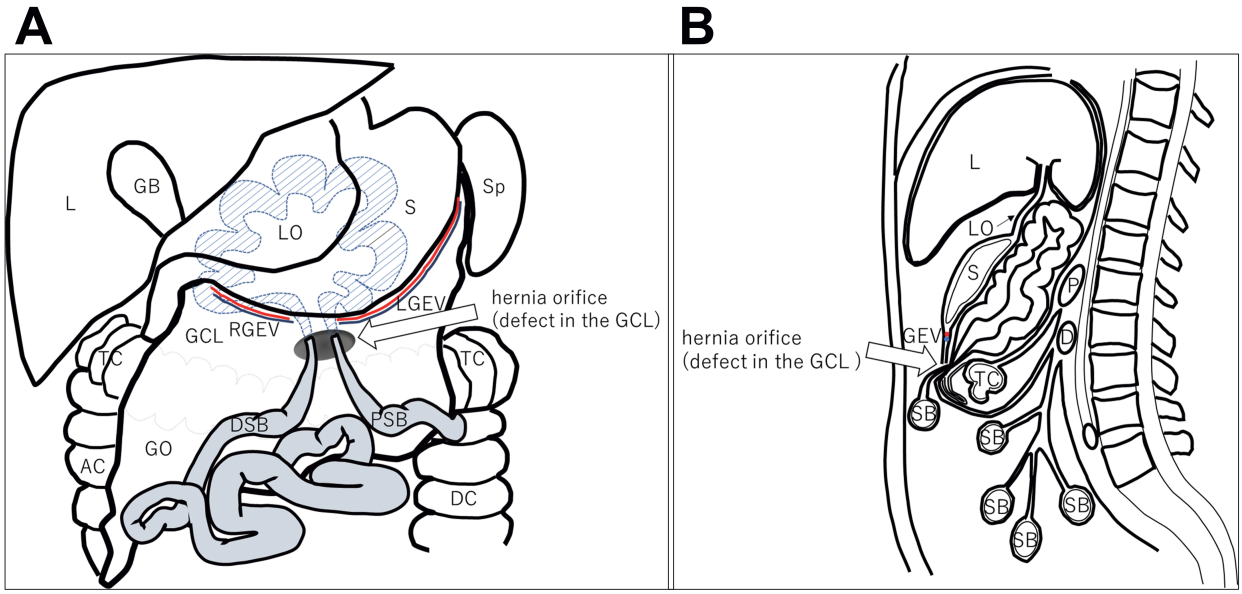

Figure 6. (A, B) Illustrations of the current case of jejunal herniation into the lesser sac through a defect in the gastrocolic ligament. (A) The coronal view. (B) The sagittal view.
AC, ascending colon; D, duodenum (horizontal segment); DC, descending colon; DSB, distal small bowel; GB, gallbladder; GCL, gastrocolic ligament; GEV, gastroepiploic vessels; GO, greater omentum (free hanging part); L, liver; LGEV, left gastroepiploic vessels; LO, lesser omentum; P, pancreas; PSB, proximal small bowel; RGEV, right gastroepiploic vessels; S, stomach body; SB, small bowel; Sp, spleen; and TC, transverse colon.

vessels through the GCL defect and incarceration in the lesser sac. These CT findings closely reflected the pathophysiology of this rare IH type, allowing preoperative diagnosis with high confidence.

The differential diagnosis of IH into the lesser sac through a defect in the GCL includes lesser sac hernia through the foramen of Winslow, lesser sac hernia through a defect in the lesser omentum, and lesser sac hernia through a defect in the transverse mesocolon[3]. The key to differentiating these distinct lesser sac hernias is to identify the hernia's orifices[3], which can be facilitated by MDCT.

In conclusion, the present case illustrates the MDCT findings of a patient with an IH entering the lesser sac through a defect in the GCL. This case highlights the utility of MDCT in the diagnosis of this rare-type IH. Knowledge of the anatomy of the omentum and lesser sac is key to correct diagnosis.

Acknowledgements

All authors have no COI to declare regarding the present case report.

Written informed consent was obtained from the patient for publication of this case report and any accompanying images.

References

1. Martin LC, Merkle EM, Thompson WM. Review of internal hernias: radiographic and clinical findings. AJR Am J Roentgenol 2006;186:703-717.
2. Takeyama N, Gokan T, Ohgiya Y, et al. CT of internal hernias. Radiographics 2005;25:997-1015.
3. Doishita S, Takeshita T, Uchima Y, et al. Internal hernias in the era of multidetector CT: correlation of imaging and surgical findings. Radiographics 2016;36:88-106.

4. Yang DH, Chang WC, Kuo WH, et al. Spontaneous internal herniation through the greater omentum. Abdom Imaging 2009;34:731-733.
5. Lee SH, Lee SH. Spontaneous transomental hernia. Ann Coloproctol 2016;32:38-41.
6. Ahn SR, Kim KY, Lee JH. Small bowel obstruction caused by spontaneous transomental hernia: a case report. Korean J Gastroenterol 2022;80:186-189.
7. Okayasu K, Tamamoto F, Nakanishi A, et al. A case of incarcerated lesser sac hernia protruding simultaneously through both the gastrocolic and gastrohepatic omenta. Radiat Med 2002;20:105-107.
8. Inoue Y, Nakamura H, Mizumoto S, et al. Lesser sac hernia through the gastrocolic ligament: CT diagnosis. Abdom Imaging 1996;21:145-147.
9. Joo YE, Kim HS, Choi SK, et al. Internal hernia presenting as obstructive jaundice and acute pancreatitis. Scand J Gastroenterol 2002;37:983-986.
10. Min JS, Lee JH, Jin SH, et al. Difficult diagnosis of a double omental hernia that led to extensive small bowel infarction. Hernia 2010;14:523-525.
11. Talebpour M, Habibi GR, Bandarian F. Laparoscopic management of an internal double omental hernia: a rare cause of intestinal obstruction. Hernia 2005;9:195-197.
12. DeMeo JH, Fulcher AS, Austin RF Jr, et al. Anatomic CT demonstration of the peritoneal spaces, ligaments, and mesenteries: normal and pathologic processes. Radiographics 1995;15:755-770.

Osaka City Med. J. Vol. 70, 35-41, 2024

Commando Operation with Aortic Root Replacement for a Patient with Extensive Infective Endocarditis Surrounding the Aortomitral Fibrous Continuity: Report of a Case

Yasuyuki Bito, Masanori Sakaguchi, Noriaki Kishimoto, Akihiro Sumiya, Takuya Miura, and Takanobu Aoyama

Department of Cardiovascular Surgery, Osaka City General Hospital

Abstract

A 16-year-old male patient with a bicuspid aortic valve developed aortic and mitral valve infective endocarditis. The vegetation was mainly in the left atrium and had spread around the intervalvular fibrous body. During surgery, we extensively excised the aortic and mitral valves with the aortomitral continuity by combining Manougian aortic enlargement with an extended transseptal incision. We replaced the mitral valve with a bioprosthetic valve and reconstructed the intervalvular fibrous body with a bovine pericardial patch. Aortic root replacement was then performed. The patient's postoperative course was uneventful, and he was discharged following additional antibiotic therapy.

Key Words: Infective endocarditis; Commando operation; Intervalvular fibrous body

Introduction

Extensive infective endocarditis with tissue destruction surrounding the aortomitral intervalvular fibrous body (IVFB) is a challenging situation for surgeons. For such patients, the Commando operation can be a practical treatment option. This procedure usually involves an extended incision in the aortic and mitral annulus combined with reconstruction of the structures surrounding the aortomitral IVFB. We herein describe a surgical case of extensive aortic and mitral infective endocarditis for which we performed the Commando operation.

Case Report

A 16-year-old male patient was referred to our institution 1 week after developing a high fever, visual field disturbance, and abnormal heart murmur. Echocardiography revealed severe aortic valve insufficiency, a possible aortic root abscess, and extensive vegetation in the left atrium (Fig. 1). *Staphylococcus aureus* was identified by a blood culture. We diagnosed the patient with aortic and mitral valve infective endocarditis, which had spread around the aortomitral continuity. Because cerebral bleeding was detected in the patient's right occipital lobe by computed tomography (Fig. 2),

Received October 17, 2023; accepted April 9, 2024.
Correspondence to: Yasuyuki Bito, MD, PhD.
Department of Cardiovascular Surgery, Osaka City General Hospital,
2-13-22 Miyakojimahondori, Miyakojima-Ku, Osaka 534-0021, Japan
Tel: +81-6-6929-1221; Fax: +81-6-6929-1090
E-mail: ybito1131212@outlook.jp

(A) (B)

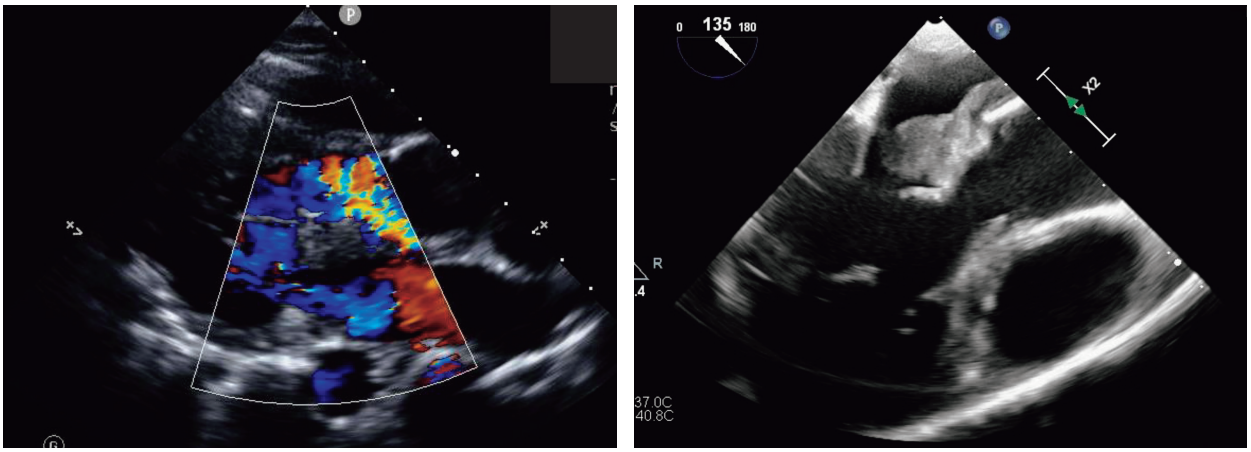

Figure 1. Echocardiography revealed severe aortic valve insufficiency (A), vegetation, and possible abscess (B).

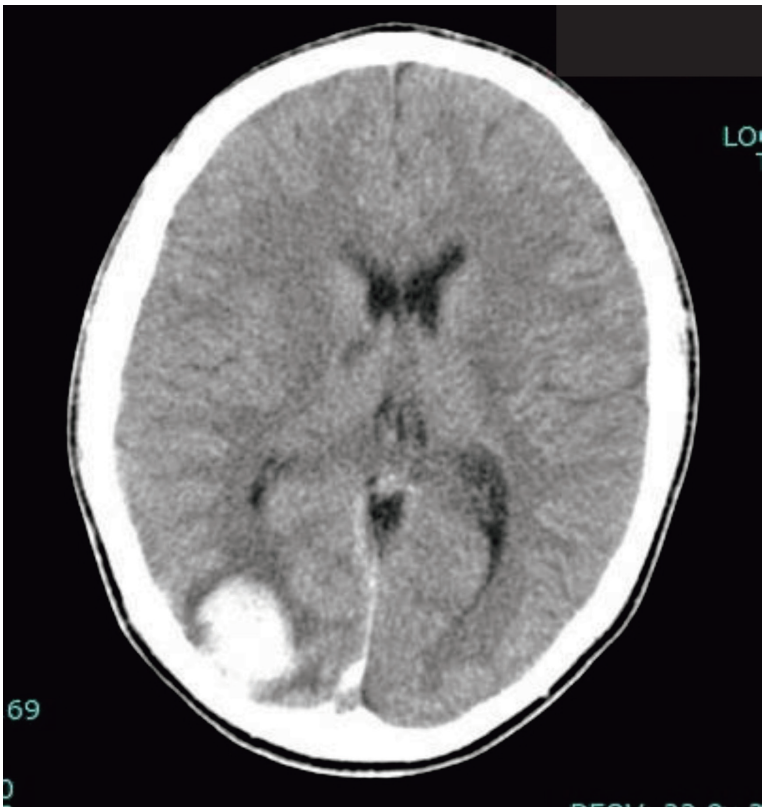

Figure 2. Computed tomography showing cerebral bleeding in the right occipital lobe.

the operation was postponed, and conservative antibiotic therapy was administered. However, the infected tissue destruction was progressing rapidly around the anterior mitral annulus, leading to severe mitral regurgitation (Fig. 3). Therefore, we decided to proceed with the operation despite the risk of worsening cerebral hemorrhage.

During the surgery, we established cardiopulmonary bypass in the usual fashion through a median sternotomy using bicaval venous cannulation with the ordinal amount of heparin. The aortic wall adjacent to the left atrial roof looked deteriorated by the infection, which made us decide to

(A) (B)

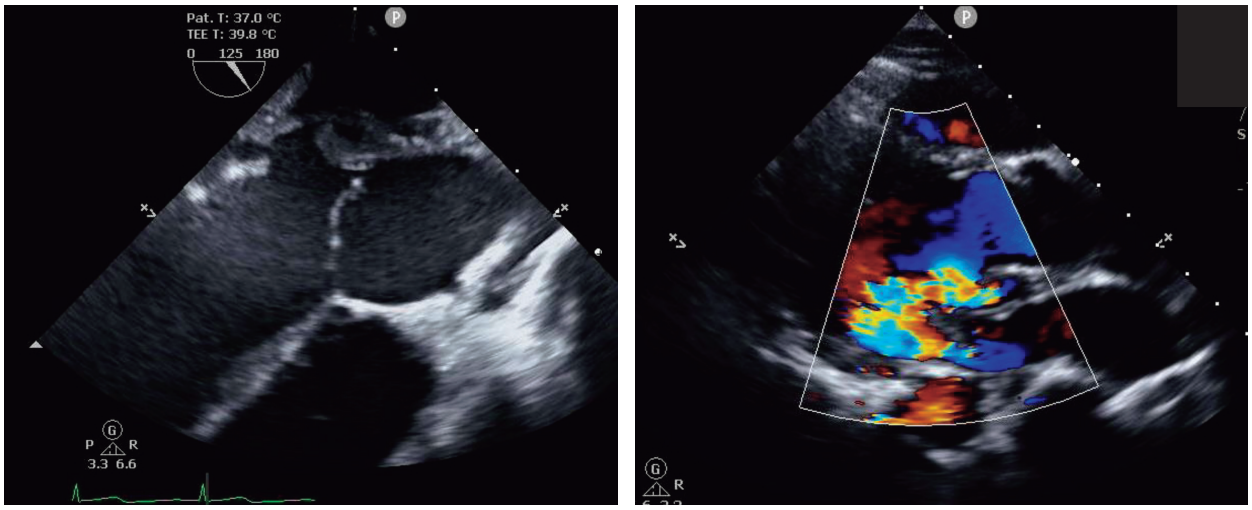

Figure 3. Tissue destruction had progressed around the intervalvular fibrous body (A), which led to severe mitral regurgitation (B).

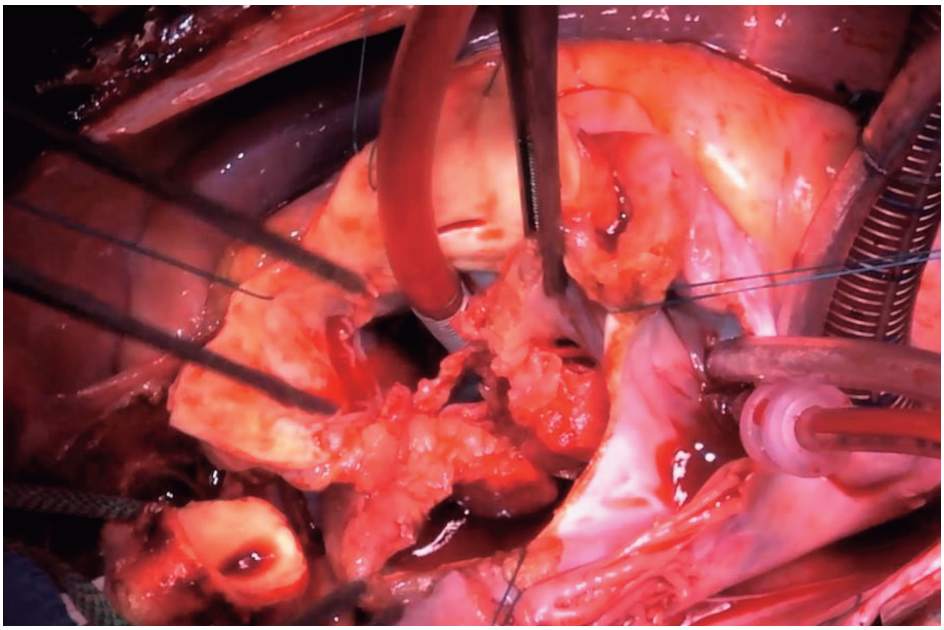

Figure 4. The infection had infiltrated around the aortomitral intervalvular fibrous body with massive vegetation.

replace the aortic root. After placing the aortic cross-clamp, we transected the ascending aorta near the sinotubular junction and found that the patient's aortic valve was a Sievers type 0 bicuspid valve. The aortic subvalvular tissue had deteriorated from one of the commissures toward the ruptured anterior mitral annulus. After resectioning the aortic valve leaflets, we made a vertical incision on the aortic wall, crossing the aortic annulus to the anterior mitral annulus. Because the left atrial wall close to the prior aortic incision was densely infiltrated by infected tissue, we made an extended transseptal incision to expose the entire massive vegetation. The infection appeared to have spread deep into the left atrial roof and the tissue surrounding the aortomitral IVFB (Fig. 4). We radically excised the vegetation, anterior mitral valve leaflets, and infected tissues, resulting in a single large

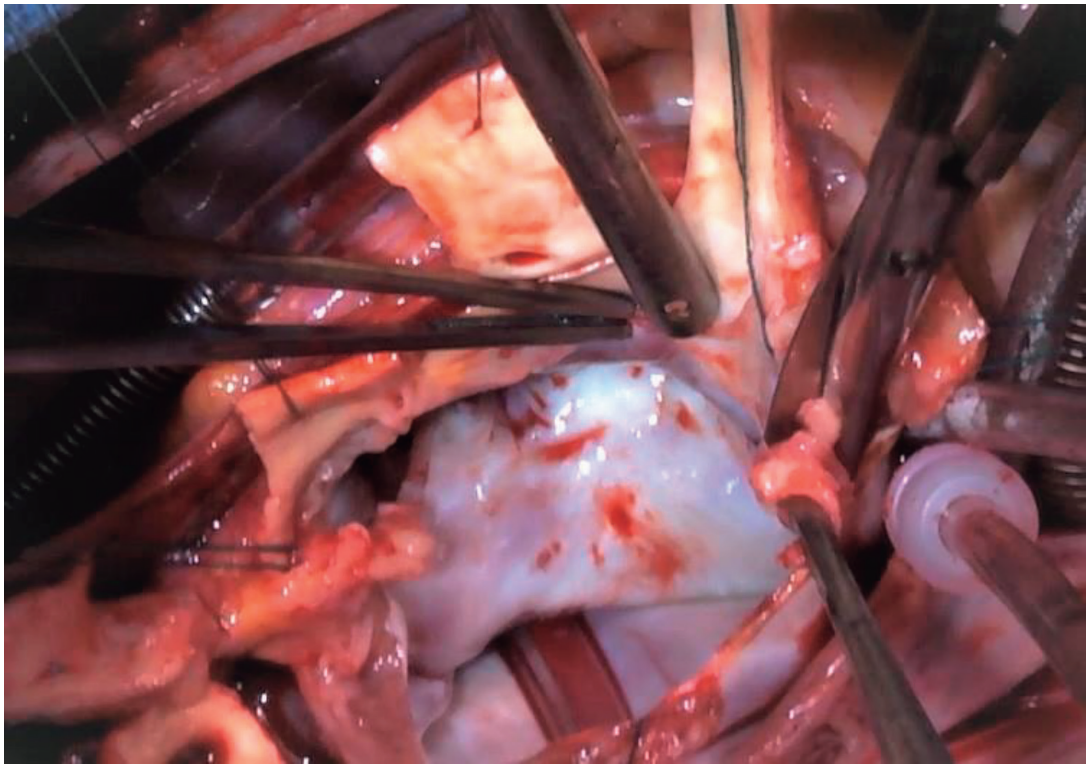

Figure 5. The large defect after debridement, including the mitral and aortic annulus.

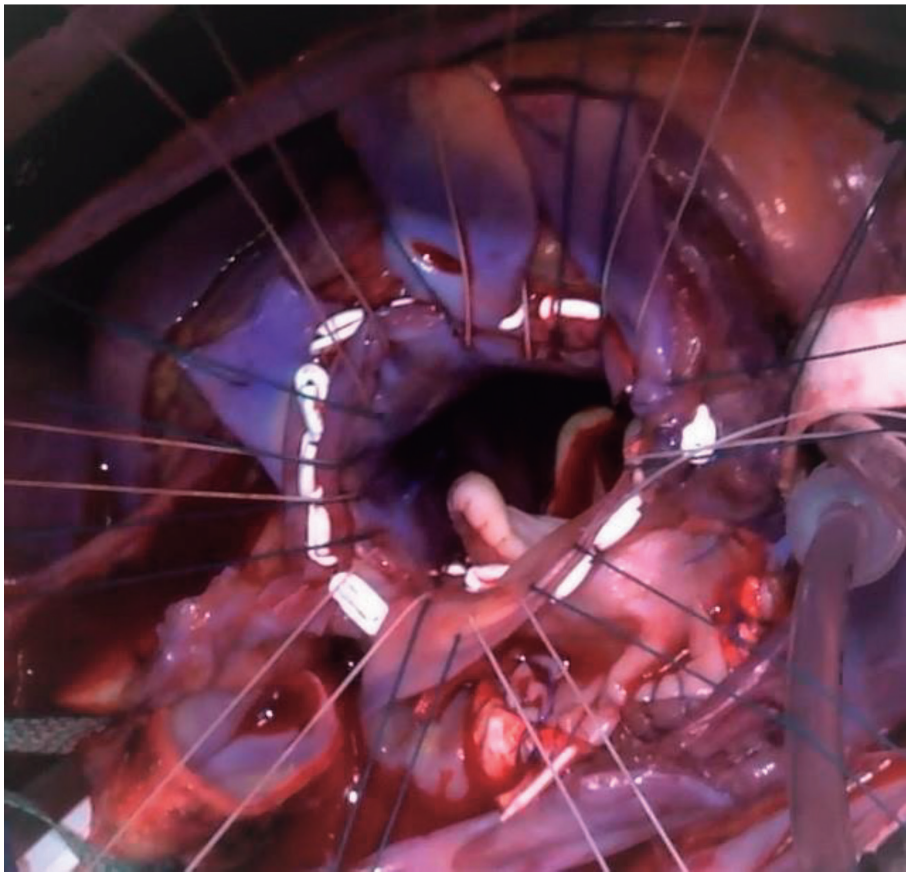

Figure 6. Aortic annulus with the reconstructed aortomitral intervalvular fibrous body.

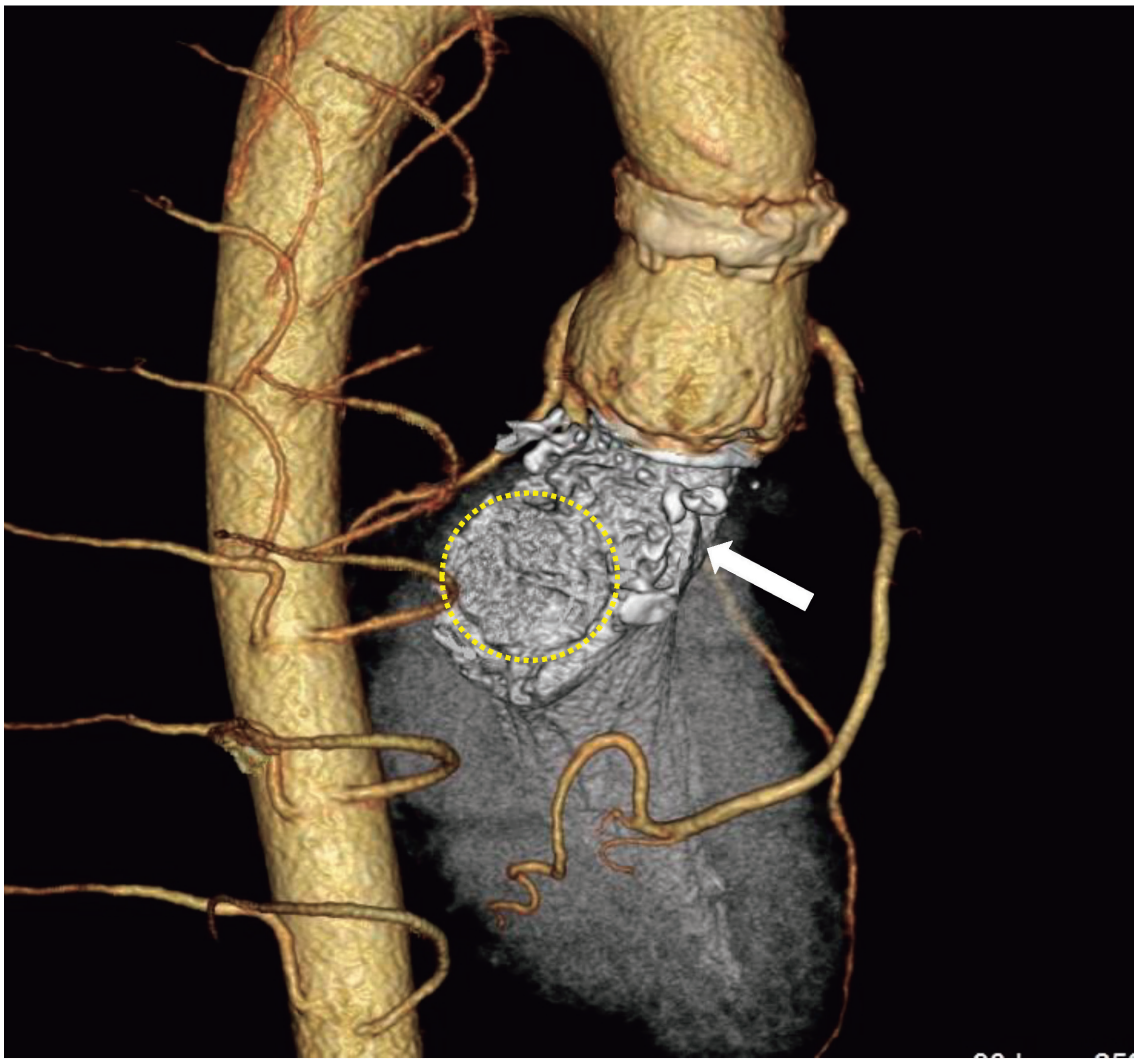

Figure 7. Postoperative computed tomography showing the reconstructed aortomitral intervalvular fibrous body (white arrow) between the aortic root and the prosthetic mitral valve (yellow dot circle).

orifice that included the aortic and mitral annulus (Fig. 5).

After placing horizontal mattress sutures on the posterior mitral annulus, we secured a bioprosthetic valve at the mitral position. A folded trimmed bovine pericardium was simultaneously affixed to the anterior prosthesis sewing ring. One tongue of the pericardium covered both the left atrial roof and the atrial septum. The other side of the folded pericardium was applied for reconstruction of the aortomitral IVFB up to the aortic valve annulus. Everted mattress sutures with pledgets were placed on the aortic annulus, including on the region of the pericardium (Fig. 6). The aortic root was replaced with a handmade composite graft with a Gelweave Valsalva graft and a bioprosthetic valve. After the cross-clamp was released, another piece of trimmed bovine pericardial patch was used to rebuild the right atrial wall.

The postoperative course was uneventful. We provided the intravenous antibiotic treatment for 6 weeks after the confirmation of the negative result from his blood culture. Computed tomography demonstrated that the patient's cerebral bleeding had not worsened and that the aortomitral IVFB was well-reconstructed (Fig. 7).

Discussion

The term "Commando operation" usually describes an operation in which the aortic and mitral valves are replaced with reconstruction of the aortomitral IVFB. David et al originally reported this operation, and their procedure was considered useful for patients with extensive infective endocarditis or severe calcification that affects the aortomitral IVFB[1]. However, this highly complex technique requires intense anatomical knowledge and occasional alterations in the surgical technique on an individual-patient basis[2]. In the present case, the infected tissue had severely infiltrated the aortomitral IVFB and the left atrial roof, and visual inspection indicated that the overall surrounding structure was affected, including the aortic root. We excised the suspicious tissue as much as possible to avoid leaving any infectious tissue. Therefore, we had no choice but to perform a Commando operation combined with aortic root replacement.

To expose the left atrium in the Commando operation, it is not always necessary to make an extended transseptal incision through the right atriotomy, as performed in this case. The left atrial roof can be opened following a Manougian incision[1]; however, in some cases, a broader view must be obtained to accomplish the operative purpose by combining the Manougian incision with the atrial septal incision, especially for patients with concomitant enhanced left atrial wall infection as in the current case[3].

We used a folded bovine pericardial patch to reconstruct the aortomitral IVFB and the left atrial roof with the atrial septum. Another option is to use two patches affixed to the anterior mitral prosthesis ring[4]. In addition, some authors have recently described a "hemi-Commando operation", in which the mitral valve is repaired[5]. This procedure can be feasible if the anterior mitral leaflet is intact, and it is especially useful for younger patients because it avoids performing mechanical mitral valve implantation. Additionally, the homograft can be suitable for the hemi-Commando procedure because the aortomitral IVFB is usually seamlessly composed in the graft with the mitral valve and aortic root[6]. Unfortunately, the anterior leaflet of the mitral valve in our patient did not appear to be preserved, and homografts are not available in our institution.

For cases of endocarditis with cerebral bleeding, it is recommended to postpone the cardiac operation for 4 weeks; otherwise, the bleeding can be lethal[7]. However, because of progressive cardiac tissue destruction in our patient, we had no choice but to perform surgery approximately 10 days after the onset of bleeding. Considering the patient's age, a mechanical valve was deemed suitable; however, because of the risk of worsening cerebral bleeding, a bioprosthesis was required to avoid intense anticoagulation during the early postoperative period.

We treated a patient with destructive infective endocarditis by performing the Commando procedure with aortic root replacement. Although the Commando operation is a complex and challenging procedure that requires surgeons to have clear anatomical images and a steady technique, it is sometimes an essential surgical option that can save patients in critical condition requiring aortomitral IVFB reconstruction.

Acknowledgements

All authors have no COI to declare regarding the present case report.

Written informed consent was obtained from the patient for publication of this case report and accompanying images.

References

1. David TE, Kuo J, Armstrong S. Aortic and mitral valve replacement with reconstruction of the intervalvular fibrous body. J Thorac Cardiovasc Surg 1997;114:766-772.
2. Misfeld M, Davierwala PM, Borger MA, et al. The "UFO" procedure. Ann Cardiothorac Surg 2019;8:691-698.
3. Guiraudon GM, Ofiesh JG, Kaushik R. Extended vertical transatrial septal approach to the mitral valve. Ann Thorac Surg 1991;52:1058-1060.
4. Marey G, Said SM. Combined Manouguian-Guiraudon approach for double valve replacement: the Commando revisited. Ann Thorac Surg 2021;111:e139-e141.
5. Vojacek J, Zacek P, Ondrasek J. Multiple valve endocarditis: a Hemi-Commando procedure. Ann Cardiothorac Surg 2019;8:705-707.
6. Navia JL, Al-Ruzzeh S, Gordon S, et al. The incorporated aortomitral homograft: a new surgical option for double valve endocarditis. J Thorac Cardiovasc Surg 2010;139:1077-1081.
7. Nakatani S, Ohara T, Ashihara K, et al. JCS 2017 Guidelines for prevention and treatment of infective endocarditis. Circ J 2019;83:1767-1809.

Instructions for Authors

The Osaka City Medical Journal will consider the publication of any original manuscript, review, case report, or short communication. Articles should be in English.

Manuscript submission. Manuscripts should be sent to the Editor, Osaka City Medical Journal, Osaka City Medical Association, Graduate School of Medicine, Osaka Metropolitan University, 1-4-3 Asahimachi, Abeno-ku, Osaka 545-8585, Japan; phone and fax 06-6645-3782; e-mail gr-med-shiigakukai@omu.ac.jp

The Journal accepts only manuscripts that contain material that has not been and will not be published elsewhere. Duplicate publication of scientific data is not permitted. If closely related papers might be considered to be duplicate publications, the possible duplicate should be submitted with the manuscript and the authors should explain in their covering letter what is original in the submitted paper. Submit three copies of the manuscript (two of which may be photocopies) together with CD-R or DVD-R containing the body text, tables and figures. The manuscript should be prepared by Microsoft Word or its compatible software (doc or docx). Acceptable formats for figures are JPG or TIF. Use only 12-point font size and a standard serif font. Double-space throughout the manuscript and use standard-sized (ISO A4, 212×297 mm) white bond paper. Make margins at least 25 mm wide on all sides. Number pages consecutively starting with the title page and ending with the reference list. Begin each of these sections on a separate page: title page, abstract, text, acknowledgements, references, tables (each one separate), and figure legends. Do not use abbreviations in the title or abstract and limit their use in the text, defining each when it first appears. Manuscripts should meet the requirements outlined below to avoid delay in review and publication. Authors whose native language is not English must seek the assistance of a native English speaker who is familiar with medical sciences. Please attach the certificate from the person(s) who edit the manuscript. Some minor editorial revision of the manuscript will be made when the editorial committee considers it necessary.

Title page. All submissions must include a title page. The full title of the paper, should be concise, specific, and informative, and should contain the message of the paper without being in sentence form. Next, include the full names and academic affiliations of all authors, and indicate the corresponding author, address, phone, fax, and e-mail address. Give a running title (not to exceed 50 characters including spaces), and three to five key words. Last, give the word count for text only, exclusive of title, abstract, references, tables, and figure legends.

Structured abstract. The abstract of 250 words or less should consist of four paragraphs headed **Background, Methods, Results,** and **Conclusions.**

Text. Full papers about experiments or observations may be divided into sections headed **Introduction, Methods, Results,** and **Discussion.**

Tables. Each table should be typed on a separate sheet in characters of ordinary size, double-spaced (with at least 6 mm of white space between lines). Each table must have a title and should be assigned an Arabic numeral ('Table 3'). Vertical rules should not be used.

Figures. For black-and-white figures, submit three original glossy prints or laser-quality proofs and three photocopies of each. One transparency and three color prints should be submitted of each color figure. Label the front of figures with the figure number. Indicate on the back of each figure the first author, the first few words of the manuscript title, and the direction of the top of the figure (if needed). Photomicrographs should have scale markers that indicate the magnification. Provide figure legends on a separate page, double-spaced, immediately after the tables. All illustrations and graphs, to be referred to as figures, should be numbered in Arabic numerals ('Fig. 2' etc.). The approximate position of each figure in the text should be indicated in the right margin of the manuscript. Illustrations in full color are accepted for publication if the editors judge that color is necessary, with the cost paid by the author.

References. Reference must be double-spaced and numbered consecutively in the order cited in the text. When listing references, follow the style of the Uniform Requirements (http://www.icmje.org/) and abbreviate names of journals according to PubMed (http://www.ncbi.nlm.nih.gov/sites/netrez). List all authors up to three; when there are four or more, list the first three and use et al.

Examples of reference style

1. Priori SG, Schwartz PJ, Napolitano C, et al. Risk stratification in the long-QT syndrome. N Engl J Med 2003;348:1866-1874.
2. Schwartz PJ, Priori SG, Napolitano C. The long-QT syndrome. In: Zipes DP, Jalife J, editors. Cardiac electrophysiology: from cell to bedside. 3rd ed. Philadelphia: W.B. Saunders; 2000. pp. 597-615.

Proofs. One set of proofs together with the original manuscript will be sent to the author, to be carefully checked for any essential changes or printer's errors. The author is requested to return the corrected proofs within 48 h of their receipt.

Short communications and case reports.

1. A short communication should have between 1500 and 2000 words, including the abstract. This word count is equivalent to about four double-spaced manuscript pages.
2. The original and two copies including three sets of figures and tables should be sent to the Editorial Office.

Manuscript submission fee. A nonrefundable fee of 10,000 JPY is due on submission of original manuscripts, case reports, and short communications. A manuscript returned beyond six months of the date of the initial decision will be considered a new submission.

Page charges. A standard publication fee of 100,000 JPY will be applied for each accepted paper. Authors are also required to pay page charge of 10,000 JPY per printed page.
Ex) If your article has 10 pages, the amount of fee is 100,000 JPY+10 pages×10,000 JPY=200,000 JPY.

Reprints. If you were interested in ordering reprints of your article, we accept at least 50 full-color copies. Authors are required to pay page charge of 100 JPY per printed page. Ex) If you request 60 copies for 10-page article, the amount of fee is 100 JPY×10 pages×60 copies=60,000 JPY.

Studies of human subjects. It is the responsibility of the authors to ensure that any clinical investigation they did and report in manuscripts submitted to the Osaka City Medical Journal are in accordance with the Declaration of Helsinki (http://www.wma.net).

Animal studies. It is the responsibility of the authors to ensure that their experimental procedures are in compliance with the "Guiding Principles in the Care and Use of Animals" (http://www.the-aps.org/pub_affairs/humane/pa_aps_guiding.htm) published each month in the information for authors of the American Journal of Physiology.

Conflict of Interest (COI) Disclosure.

1. It is the responsibility of the authors to disclose any COI by signing the form.
2. If the authors have no conflicts, please state "All authors have no COI to declare regarding the present study" in the Acknowledgements.
   Authors are required to disclose any relationships with company or organization (such as funds, consultancy fee, grant, fee for speaking, stock or shares). At the time of initial submission, the corresponding author is responsible for obtaining conflict of interest information from all authors.

[Revised: June 8, 2021]

COPYRIGHT TRANSFER AND STATEMENT OF ORIGINALITY

We approve the submission of this paper to the Osaka City Medical Association for publication and have taken to ensure the integrity of this work. We confirm that the manuscript is original and does not in whole or part infringe any copyright, violate any right of privacy or other personal or priority right whatever, or falsely designate the source of authorship, and that it has not been published in whole or in part and is not being submitted or considered for publication in whole or in part elsewhere (abstracts excluded).
We agree to transfer copyright the manuscript entitled

_____

_____

to the Osaka City Medical Association upon its acceptance for publication.

Write clearly and signature

(Author: print or type)	(Signature)	(Date)
(Author: print or type)	(Signature)	(Date)
(Author: print or type)	(Signature)	(Date)
(Author: print or type)	(Signature)	(Date)
(Author: print or type)	(Signature)	(Date)
(Author: print or type)	(Signature)	(Date)
(Author: print or type)	(Signature)	(Date)
(Author: print or type)	(Signature)	(Date)
(Author: print or type)	(Signature)	(Date)
(Author: print or type)	(Signature)	(Date)

OCMJ for Conflict of Interest (COI) Disclosure Statement

The purpose of this form is to provide readers of your manuscript with information about your other interests that could influence how they receive and understand your work. The form is designed to be completed and stored electronically. Each author should submit this form and is responsible for the accuracy and completeness of the submitted information.

1. 1) Have you accepted from a sponsor or any company or organization (More than 1,000,000 JPY per year from a specific organization) ? (Please circle below)

   (1) Funds ? ..... Yes / No

   (2) Consultancy fee ? ..... Yes / No

   (3) Any grant ? ..... Yes / No

   (4) Fee for speaking ? ..... Yes / No

   2) Do you hold any stock or shares related to the manuscript ?

   (1) Directly ? ..... Yes / No

   (2) Indirectly, via family members or relatives ? ..... Yes / No

   3) If any of above items are "yes", please provide detailed information below.

2. If none of the above apply and there is no COI please clearly state "All authors have no COI to declare regarding the present study".

Manuscript Title:

Name / Signature_____ **Date**_____

Manuscript Identifying Number (if you know it):

Editorial Committee

Yukio Miki, MD (Chief Editor)

Yasuhiro Fujiwara, MD
Wakaba Fukushima, MD
Takeo Goto, MD
Yoshikazu Hiura, MD
Masayuki Hosoi, MD
Koki Inoue, MD
Kenichi Kohashi, MD
Makoto Kondo, MD
Kenji Mizuseki, MD
Atsushi Shioi, MD
Toshiyuki Sumi, MD
Kishiko Sunami, MD
Junji Uchida, MD

The volumes and issues published in 1954-2018 were as follows: Vol 1 (one issue), Vols 2-5 (2 issues, each), Vols 6-7 (one issue, each), Vols 8-9 (2 issues, each), Vol 10 (one issue), Vol 11 (2 issues), Vol 12 (one issue), Vol 13 (2 issues), Vols 14-20 (one issue, each), Vol 21 (2 issues), Vol 22 (one issue), Vols 23-65 (2 issues, each), Vol 66 (one issue), Vol 67-69 (2 issues, each)

Publisher : Osaka City Medical Association,
Graduate School of Medicine, Osaka Metropolitan University
1-4-3 Asahimachi, Abeno-ku, Osaka 545-8585, Japan